2016-12-30

Inhibition of Ubc13-mediated ubiquitination by GPS2 regulates multiple stages of B cell development

THE JOURNAL OF BIOLOGICAL CHEMISTRY VOL. 292, NO. 7, pp. 2754–2772, February 17, 2017

Inhibition of Ubc13-mediated Ubiquitination by GPS2 Regulates Multiple Stages of B Cell Development*[S]

Received for publication, August 24, 2016, and in revised form, December 21, 2016 Published, JBC Papers in Press, December 30, 2016, DOI 10.1074/jbc.M116.755132

Claudia Lentucci[‡], Anna C. Belkina[§¶1], Carly T. Cederquist[‡1], Michelle Chan[‡], Holly E. Johnson[‡], Sherry Prasad[‡], Amanda Lopacinski[‡], Barbara S. Nikolajczyk[¶], Stefano Monti[‖], Jennifer Snyder-Cappione[§¶], Bogdan Tanasa[**], M. Dafne Cardamone[‡], and Valentina Perissi[‡2]

From the Departments of [‡]Biochemistry, [¶]Microbiology, and [‖]Medicine and the [§]Flow Cytometry Core Facility, Boston University School of Medicine, Boston, Massachusetts 02118 and the [**]Department of Pediatrics, Stanford University School of Medicine, Stanford, California 94305

Edited by George N. DeMartino

Non-proteolytic ubiquitin signaling mediated by Lys[63] ubiquitin chains plays a critical role in multiple pathways that are key to the development and activation of immune cells. Our previous work indicates that GPS2 (G-protein Pathway Suppressor 2) is a multifunctional protein regulating TNFα signaling and lipid metabolism in the adipose tissue through modulation of Lys[63] ubiquitination events. However, the full extent of GPS2-mediated regulation of ubiquitination and the underlying molecular mechanisms are unknown. Here, we report that GPS2 is required for restricting the activation of TLR and BCR signaling pathways and the AKT/FOXO1 pathway in immune cells based on direct inhibition of Ubc13 enzymatic activity. Relevance of this regulatory strategy is confirmed *in vivo* by B cell-targeted deletion of GPS2, resulting in developmental defects at multiple stages of B cell differentiation. Together, these findings reveal that GPS2 genomic and non-genomic functions are critical for the development and cellular homeostasis of B cells.

Protein ubiquitination represents a key regulatory strategy for controlling both innate and adaptive immune responses (1–3). Ubiquitination is a reversible modification that is achieved via the sequential actions of several classes of enzymes, including an ubiquitin (Ub)-activating[3] enzyme (E1), an Ub-conjugating enzyme (E2), and an Ub ligase (E3) (4, 5). Polyubiquitination of target proteins with chains of different topology can promote either protein degradation or serve, as in the case of other post-translational modifications, to influence protein functions and interactions (6, 7). Among others, the Lys[63]-linked ubiquitin chains synthesized by the E2-conjugating enzyme Ubc13 are non-proteolytic (8). In innate immunity, non-proteolytic ubiquitination events play a central role in multiple signaling pathways activated by the recognition of early response cytokines and infectious agents via cell surface or intracellular receptors (9–13). These include the TNF receptor (TNFR) superfamily, the Toll-like receptors (TLRs), NOD-like receptors (NLRs), and RIG-I-like receptors (RLRs). Similarly, activation of the B cell antigen receptors (BCRs) and T cell receptors (TCRs) during adaptive immune responses results in the activation of complexes that rely on Lys[63] ubiquitination for signal transduction (1, 3, 14–20). These ubiquitination events represent key nodes in the tight regulation of immune responses as indicated by the fact that multiple negative regulators impinge on these steps. These regulatory factors are often deubiquitinases (*i.e.* A20/TNFAIP3, CYLD, and the newly identified MYSM1) that help control the signal specificity and prevent the aberrant constitutive activation of pro-inflammatory responses by removing polyubiquitin chains from their substrates (1, 21–24). Importantly, genetic deletion experiments have confirmed their anti-inflammatory functions *in vivo*, and loss of negative regulation is consistently found associated with hyperactivation of downstream signaling mediators, including IKK and NF-κB (25–27). Also, based on frequent inactivation by deletions or somatic mutations in B cell lymphomas, A20/TNFAIP3 is described as a tumor suppressor required for preventing the constitutive activation of NF-κB signaling that is often used in hematological malignancies as a pro-survival strategy (28–31).

GPS2 (G-protein Pathway Suppressor 2) was originally identified while screening for suppressors of Ras activation in the yeast pheromone response pathway (32). Recent studies by our lab and others indicate that GPS2 plays an important anti-inflammatory role in adipose tissue and macrophages and is required for the expression of genes regulating cholesterol and triglyceride metabolism in liver and adipose tissue (33–38). Because of the multiple functional interactions observed

* This work was supported by awards from the Grunebaum Cancer Foundation and the Genomic Science Institute at Boston University and National Institutes of Health Grant R01DK100422 (to V. P.) and by a seed grant from the Medicine Department at Boston University School of Medicine (to V. P. and S. M.). This work was also supported by a National Research Service Award (NRSA) Individual Predoctoral Fellowship from the National Institutes of Health (F31DK108571) (to C.T.C.). The authors declare that they have no conflicts of interest with the contents of this article. The content is solely the responsibility of the authors and does not necessarily represent the official views of the National Institutes of Health.

[S] This article contains supplemental Tables S1–S3.

The RNAseq data are available in the GEO database under accession number GSE92751.

[1] These authors contributed equally to this work.

[2] To whom correspondence should be addressed: Biochemistry Dept., Boston University School of Medicine, Silvio Conte Bldg., Boston, MA 02118. Tel.: 617-638-4115; Fax: 617-638-5339; E-mail: vperissi@bu.edu.

[3] The abbreviations used are: Ub, ubiquitin; TNFR, TNF receptor; TLR, Toll-like receptor; BCR, B cell antigen receptor; MZ, marginal zone; DE, differentially expressed; FC, -fold change; IPA, Ingenuity Pathway Analysis; qPCR, quantitative PCR; FO, follicular; H&E, hematoxylin and eosin; ILB, innate-like B cell; Gardi, gardiquimod; HTLV, human T cell leukemia virus; IP, immunoprecipitation; WB, Western blotting; BM, bone marrow; mTOR, mechanistic target of rapamycin.

between GPS2 and transcriptional regulators, including the NCoR/SMRT corepressor complex, the histone acetyltransferase p300, and numerous DNA-binding transcription factors, GPS2 activity has been mainly studied in the context of its nuclear functions, including both transcriptional repression and activation (33–35, 37, 39–46). However, our recent work has also identified a non-transcriptional role for GPS2 in the cytoplasm, specifically linking GPS2 with the modulation of the TNFα signaling pathway and the activation of JNK (33). Interestingly, our findings reveal that distinct GPS2 functions in different cellular compartments rely on a conserved regulatory strategy based on the inhibition of ubiquitin-conjugating complexes that are responsible for the formation of non-degradative Lys^{63} ubiquitin chains (TRAF2/Ubc13 in the cytosol and RNF8/Ubc13 in the nucleus) (33, 37). This raises the questions of whether GPS2 inhibition of Ubc13-dependent ubiquitination events extends to other signaling pathways and to what extent GPS2-mediated regulation of ubiquitin signaling is required *in vivo* for the development and homeostasis of immune cells.

Here, we have addressed these questions using B cell-targeted deletion of GPS2 in mice. Our results indicate that in B cells, GPS2 regulates both the AKT/FOXO1 pathway and the TLR and BCR signaling pathways via direct inhibition of Ubc13 enzymatic activity. *In vivo*, GPS2 deletion results in a partial block in the maturation of bone marrow B cells past the pre-B cell stage and a significant decrease in splenic marginal zone (MZ) B cells and peritoneal and splenic B-1 cells caused by synergistic transcriptional and non-transcriptional effects.

Results

Generation of B Cell-specific GPS2 Knock-out (GPS2-BKO) Mice—GPS2 plays a key anti-inflammatory role in both liver and adipose tissue (33, 35, 36). Its relatively high expression levels in human spleen and leukocyte cells suggest that it could also play an important role in regulating immune cell functions (47). However, its relevance in this context has not yet been investigated. To overcome the early embryonic lethality of global GPS2 deletion (45) and investigate GPS2 relevance in the regulation of B cells functions and development, we chose a conditional deletion approach. Mice specifically deleted for GPS2 in the B cell lineage were generated by crossing $GPS2^{fl/fl}$ mice, carrying LoxP sites flanking exon 3–6, with hemizygous CD19-Cre mice (The Jackson Laboratory). Although insertion of Cre disrupts the CD19 coding sequence, leading to a CD19 deficiency in the homozygous situation, the CD19-$Cre^{+/Cre}$ mice are phenotypically normal and can be used for B lineage-specific deletion (48). Overall, $GPS2^{fl/fl}$-$Cre^{+/Cre}$ (GPS2-BKO) mice are viable, healthy, and fertile. To confirm the specificity and efficacy of our deletion strategy, B cells were isolated from the spleens of WT and GPS2-BKO littermates by negative selection. Visual observation of the spleens did not reveal any gross anatomical differences, as confirmed by a comparable splenic index (Fig. 1*A*). Comparable numbers of total splenocytes and isolated B cells were obtained from GPS2-BKO mice and WT littermates (Fig. 1, *B* and *C*). GPS2-specific deletion in the B cell lineage was confirmed through genomic PCR analysis, quantitative RT-PCR, and Western blotting of the B cell-positive and B cell-negative splenocyte fractions (Fig. 1, *D–F*).

Gene Expression Profiling of Splenic B Cells by RNA Sequencing—Based on the proposed role of GPS2 as both a regulator of cytosolic signaling pathways and a transcriptional cofactor for multiple transcription factors (34, 36, 37, 43, 45, 46), we predicted that GPS2 deletion might have a broad effect on the B cell transcriptome. To investigate the full profile of GPS2-regulated genes in our experimental model, we performed an open-ended transcriptomic analysis of the splenic B cells isolated from WT and GPS2-BKO littermates by RNA-Seq. Bioinformatic analysis of the RNA sequencing results revealed 716 differentially expressed (DE) genes (with 5% false discovery rate threshold) that were consistently identified in three biological replicates profiled in distinct sequencing experiments (either using Illumina or NEB kits for generating the cDNA library). Among the DE genes, 198 were found to be up-regulated, and 518 were found to be down-regulated (FC $>$ 1.1) in GPS2-deficient cells, with *GPS2* being, as expected, the most down-regulated gene (FCs between -2.5 and -3.2) (Fig. 1*G* and supplemental Table S1).

Based on our previous work showing an inhibitory role for GPS2 toward TRAF2-dependent activation of the TNFR1 pathway (33), we expected the loss of GPS2 to associate with the up-regulation of genes downstream of TRAF2 and TNFα signaling. In agreement with this hypothesis, pathway analysis for potential upstream regulators of the DE genes predicted TRAF2/3 (activation score = 2.449) and MAP4K4 (activation score = 2.714) to be up-regulated (supplemental Table S2). However, GO analysis of the biological processes and cellular and molecular functions associated with the DE genes revealed a significant enrichment in terms associated with ribosomal activity, protein translation, and mitochondrial functions rather than terms related to inflammation or immune-specific functions (graph in supplemental Table S3). Accordingly, with this analysis, the mTORC2 complex subunit RICTOR was also enriched among the potential upstream regulators of the DE genes (activation score = 4.123) (supplemental Table S2), and top canonical pathways associated with the DE genes (as identified by IPA analysis) included EIF2 signaling, mitochondrial dysfunction, and mTOR signaling (Fig. 1*H*). Together, these analyses confirmed unpublished observations in other cell models that support a general role for GPS2 in regulating energy metabolism in cells (111).[4] More specifically relevant to the B cell model of this signature, IPA analysis of the top diseases and biological functions that are potentially affected by this altered gene expression profile predicted defects in "hematological system development and function" in GPS2-BKO mice, including an arrest in B-lymphocytes development and differentiation characterized by a potential decrease in "quantity of B-1 lymphocytes" and "quantity of marginal-zone B lymphocytes" and an increase in "pre-B lymphocytes" (Fig. 1*I* and supplemental Table S4).

Defective B Cell Development in the Bone Marrow of GPS2-deficient Mice—Based on these predictions, we investigated whether GPS2 deletion affects B cell development. To assess for potential defects during the maturation of B cells, we quantified

[4] M. D. Cardamone and V. Perissi, unpublished data.

B cell subsets in WT and GPS2-BKO. For this we developed a 13-color multicolor flow cytometry panel that allowed us to identify developing B cell subsets in the bone marrow (pre pro B cells, pro B cells, pre B cells, immature B cells, and transitional B cells), the spleen (B-1a and B-1b; transitional T1, T2, and T3; marginal zone and marginal zone T2 precursors; and follicular B cells), and the peritoneal cavity (B-1a, B-1b, and conventional B-2 cells).

The total numbers of cells recovered from the bone marrow was not affected by GPS2 deletion (Fig. 2*A*). Overall, the expres-

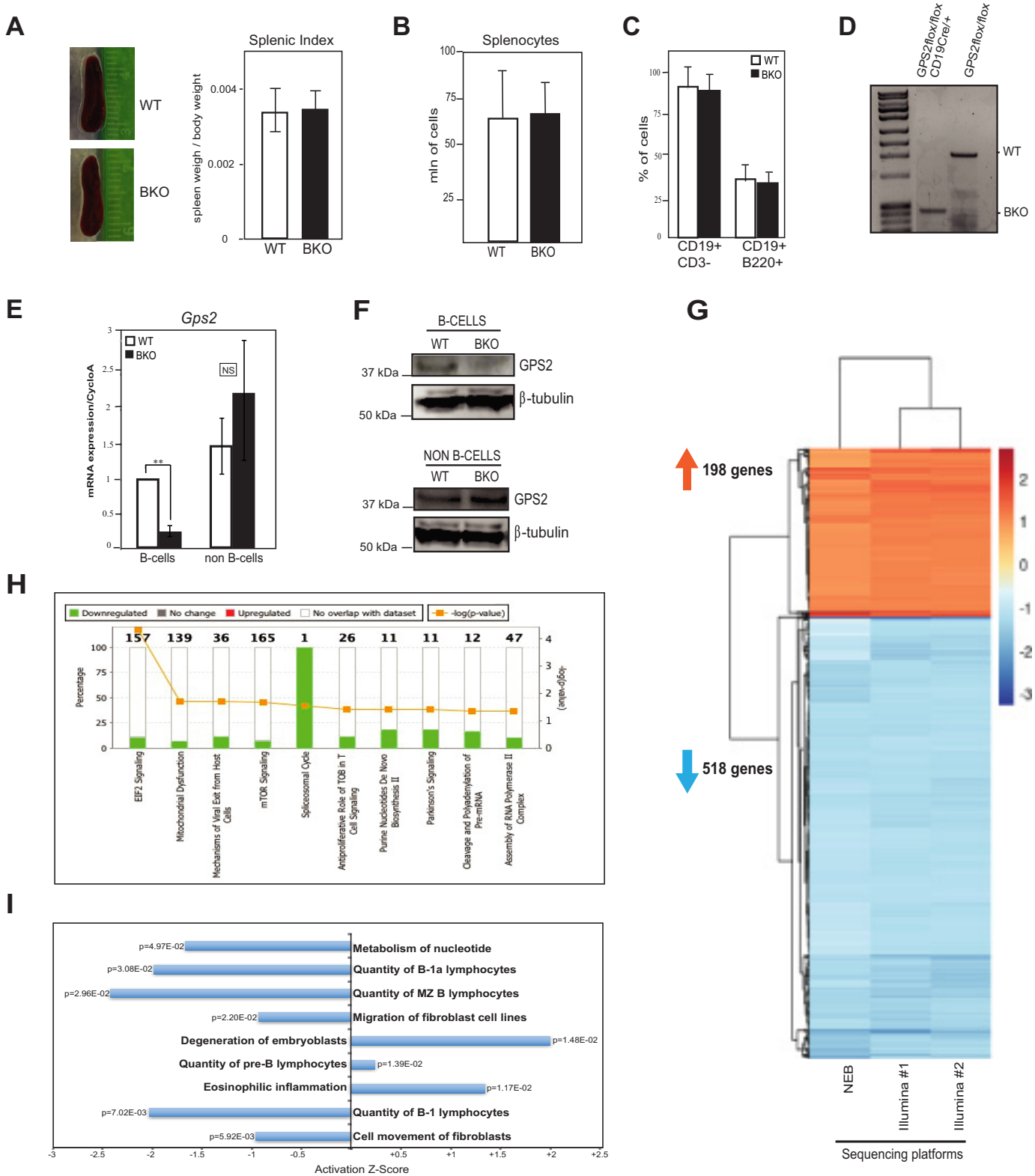

sion of B cell markers in the bone marrow corresponded to a normal B cell phenotype (Fig. 2*B*), but the frequency of mature B cells was slightly reduced in GPS2 mutant mice relative to wild type as indicated by a decrease in IgM^+ cells and a corresponding increase in $B220^+IgM^-$ populations (Hardy's Fractions B-D) (Fig. 2*C*). In particular, we observed a significant increase in the frequency of $B220^{low}CD19^+CD93^+CD43^-IgM^-$ B cells (pre-B cells, Hardy's Fraction D). In the IgM^+ subset, it was the $B220^{high}CD19^+CD93^-CD23^+IgD^+$ transitional B cell population (Hardy's fraction F) that was decreased, whereas the immature B cells ($B220^{high}CD19^+CD93^+CD23^-IgD^-$, fraction E) were comparable in WT and GPS2-BKO mice (Fig. 2*D*). Together these results reveal that the development of GPS2-BKO cells is impaired at the pre-BCR stage of the B cell maturation process in the bone marrow. Interestingly, a similar phenotype is promoted by the deletion of FOXO1 in pre-B/immature cells. Although earlier deletion of FOXO1 results in a block in B cell development at the pro-B cell stage, CD19-Cre-driven deletion of FOXO1 is associated with a later impairment at the pre-B cell stage, defective light κ chains rearrangement, and a lower number of recirculating mature cells (49). Among the genes significantly altered in splenic GPS2-BKO cells, the pre-BCR adaptor protein BLNK/SLP-65, the MAPK-activated kinase MK5, and the recombination activating gene RAG1 were all known to play key roles in FOXO1-mediated regulation of the rearrangement of immunoglobulin chains (50–56) (supplemental Table S1). This prompted us to investigate the possibility that lack of GPS2 affects the early stages of B cell differentiation through defective transcriptional regulation of key FOXO1 target genes. To confirm this hypothesis, we first measured by RT-qPCR analysis the expression of GPS2 putative target genes in B cell precursors isolated from the bone marrow of WT and GPS2-BKO mice. *GPS2* gene deletion driven by the CD19-Cre proved less efficient in the bone marrow than the spleen (Fig. 2*E*), as expected based on the fact that CD19-Cre efficiency of recombination has been reported as close to 90% in mature B cells, 40% in immature B and pre-B cells, and less than 5% in pro B cells (57). However, this down-regulation was sufficient to drive a significant decrease in the expression of FOXO1 target genes *RAG1*, *RAG2*, and *BLNK* (Fig. 2*F*). Interestingly, the expression of *FOXO1* gene itself was also found significantly down-regulated in GPS2-depleted cells (Fig. 2*F*). Thus, we asked whether GPS2 regulated the transcription of these genes directly or indirectly through FOXO1-mediated transcriptional events. Results of our ChIP analysis revealed significant GPS2 binding to the promoters of *BLNK*, *RAG1*, *RAG2*, and *FOXO1* genes in B cells isolated from the bone marrow (Fig. 2*G*), thus suggesting a direct role for GPS2 in the transcriptional forward loop that regulate FOXO1 and some of its target genes in developing B cells. Interestingly, FOXO1 binding on each of these promoters was drastically reduced in GPS2-BKO cells (Fig. 2*H*). Although FOXO1 binding to chromatin is unlikely to require promoter priming via histone demethylation as previously reported for PPARγ (37), it is well known that FOXO factors are negatively regulated by the PI3K/AKT pathway via phosphorylation and nuclear exclusion (50). Because we recently reported that GPS2 deletion in adipocytes leads to constitutive AKT activation (111), we asked whether GPS2-mediated regulation of AKT is conserved in B cells. Indeed, as shown in Fig. 2*I*, AKT phosphorylation was found to be increased in GPS2-BKO cells. Also, as expected in presence of enhanced AKT activation, we observed a striking up-regulation of FOXO1 phosphorylation, which is consistent with the loss of FOXO1 binding to DNA in GPS2-deficient cells (Fig. 2*I*).

In conclusion, GPS2 deletion in the mid-late stages of bone marrow differentiation causes a mild defect in the transition from pre-B to immature B cells. In particular, our data indicate that GPS2 is required during this developmental transition for the expression of a number of genes that play a key role in the recombination of immunoglobulin chains and receptor editing. Intriguingly, GPS2 appears to regulate these genes through combinatorial genomic and non-genomic functions, including direct transcriptional regulation via promoter binding and indirect regulation of the PI3K/AKT pathway. This may be a regulatory strategy conserved among distinct cell types as indicated by our recent work about the role of GPS2 in the regulation of insulin signaling in the adipose tissue and by previous ChIP-Seq data showing GPS2 binding to the FOXO1 promoter in both human 293 cells and mouse 3T3-L1 adipocytes (33, 37, 111) (Fig. 2*J*).

Targeting GPS2 Disrupts the B1 and MZ B Cell Compartments—To further characterize the development of B cells in GPS2-BKO mice, we followed the maturation pathway of B cells in the spleen, where they differentiate into either follicular (FO) or MZ B cells. FO cells represent the majority of mature B-2 cells circulating through blood and secondary lymphoid organs, whereas MZ cells are non-circulating mature B-2 cells residing in the marginal zone of splenic follicles (58). Macroscopically, there was no difference in spleen size between the animal groups, and the cell yield was consistently comparable (Fig. 1*B*). However, the cellular composition of the splenocyte populations was dramatically different (Fig. 3*A*). Resolution of the three different subsets of immature AA41+ B-2 cells did not reveal any defect in the transition from

FIGURE 1. **Generation of B cell-specific GPS2 knock-out (GPS2-BKO) mice.** *A*, Spleen's morphology and splenic index from WT and GPS2-BKO mice calculated as spleen weight/total body weight ± S.D.; data are representative of $n = 14$ female mice, age 10–16 weeks old. *B*, cell yield obtained from spleen preparations. *C*, flow cytometric analysis of B cells purity after Pan B cell isolation from total splenocytes. *D–F*, validation of GPS2 deletion in GPS2-BKO mice. *D*, PCR analysis of genomic DNA from $GPS2^{flox/flox}$ mice expressing or not expressing one copy of the *Cre* transgene under control of the CD19 promoter. *E*, RT-qPCR analysis of *Gps2* gene expression. *F*, WB for GPS2 (C-terminal antibody) on total cell lysates from B cells isolated by negative selection from total splenocytes and non-B cell splenocytes (column flow through). Bar graphs represent the sample means of three independent experiments ± S.D. *, $p < 0.05$; **, $p < 0.01$. *G*, heat map showing differentially expressed genes (FC > 1.1) in B cells from spleens of WT and GPS2-BKO mice. The results from three independent biological replicates and separate RNA-Seq experiments are shown, including two cDNA libraries generated with Illumina TruSeq stranded total RNA sample prep kit (Illumina 1 and 2) and one with NEBNext ultra directional library preparation kit (NEB). The heat map was produced using heatmap.2() functions in R and based on Minkoski distance. See supplemental Table S1 for complete list of DEGs and supplemental Table S2 for upstream regulatory networks. *H*, top canonical pathways associated with the DE genes by IPA analysis. *I*, IPA analysis of DEGs showing a selection of the top biological function potentially affected in GPS2-KO mice based on their activation Z-score. See supplemental Table S4 for the complete list.

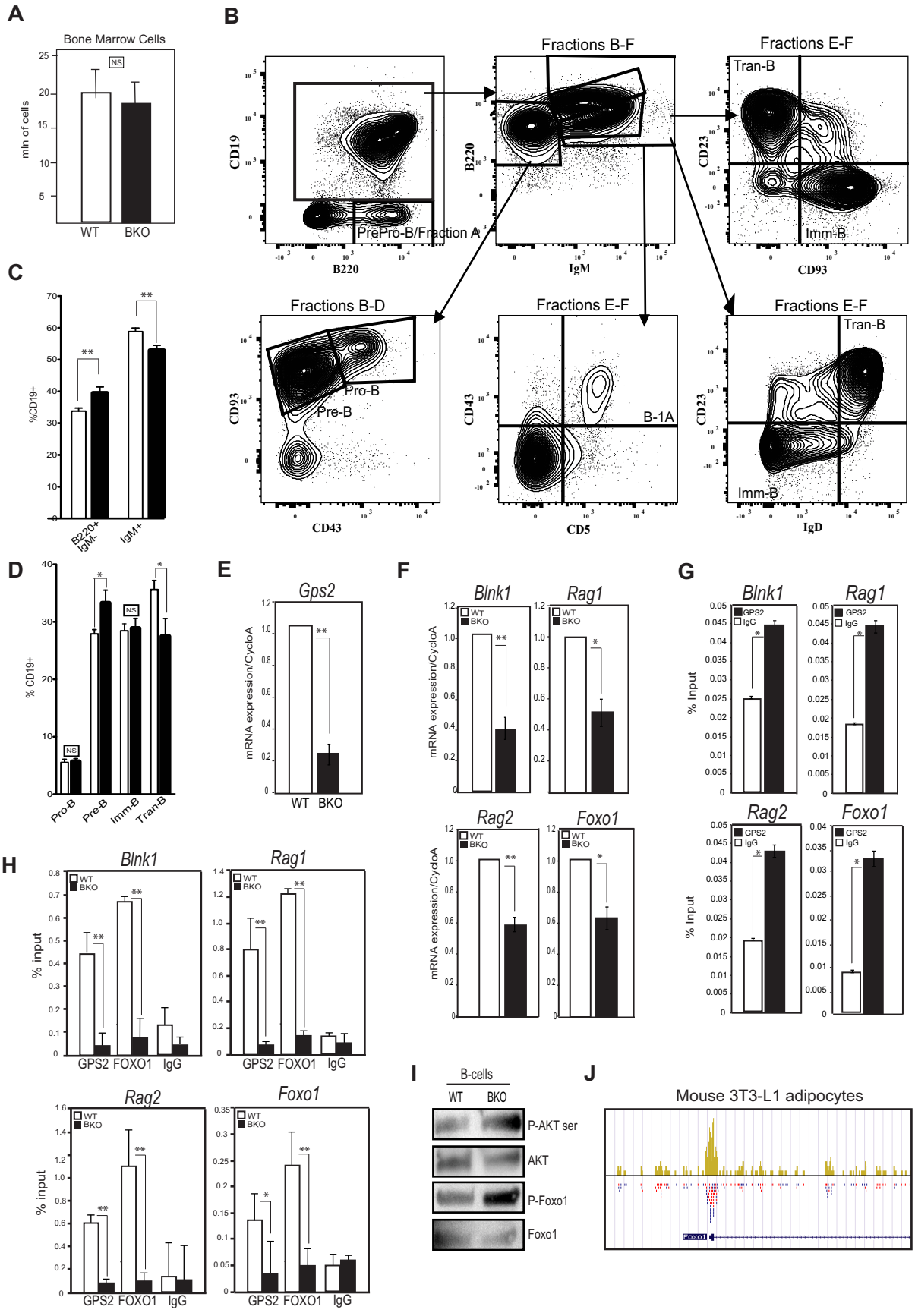

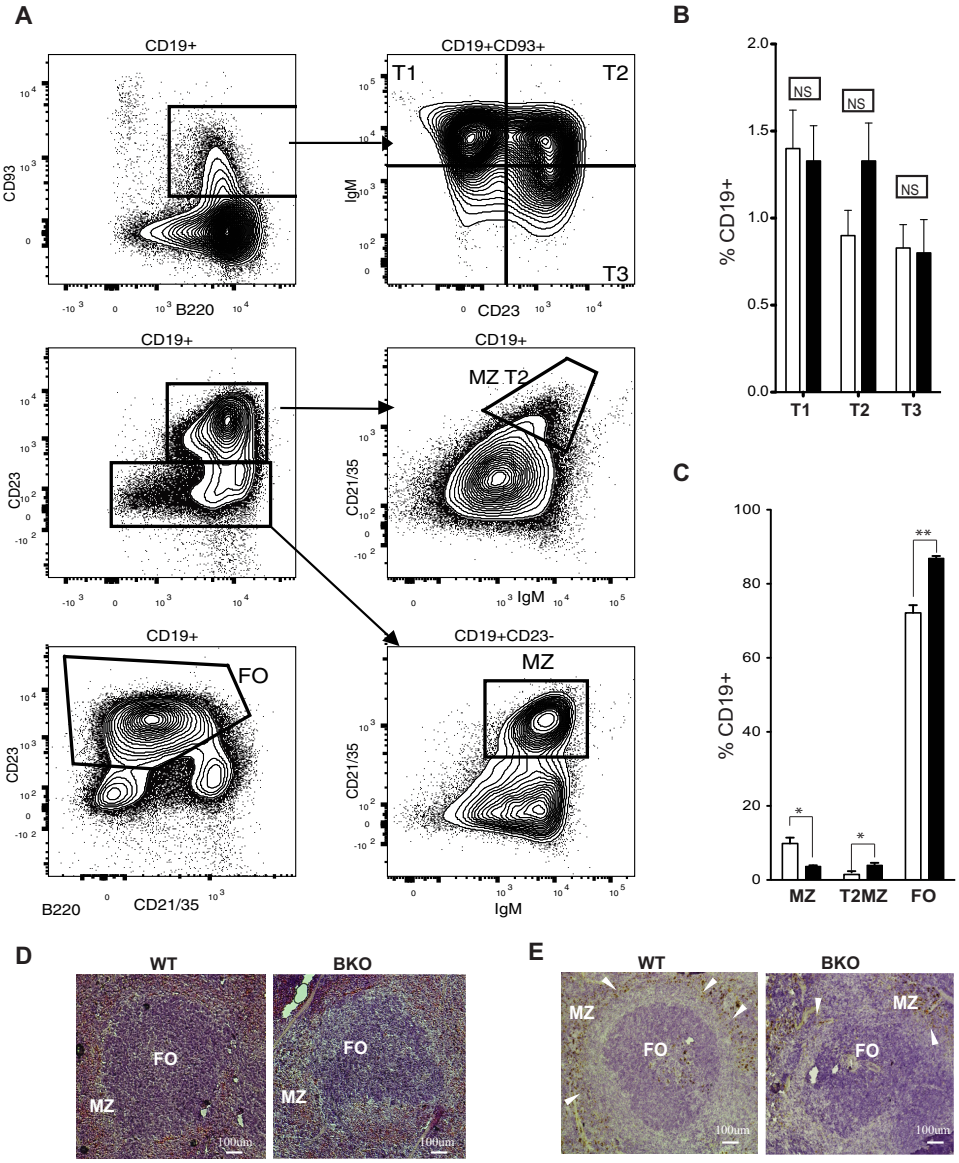

FIGURE 3. **Targeting GPS2 disrupt MZ B cell compartments.** *A*, flow cytometry analysis and gating strategy. Representative plots are shown, and cells are pregated as described above. *T1*, *T2*, and *T3*, transitional B cell subpopulations; *MZ*, marginal zone B cells; *FO*, follicular B cells. *B*, flow cytometry showing the three different subset of transitional Immature AA4.1+ B-2 cells (*T1*, *T2*, and *T3*, transitional B cell subpopulations) among $CD19^+$ cells. *C*, splenic B cell subpopulation comparison. *White bars*, WT; *black bars*, GPS2-BKO ($n = 7$). Bar graphs are ± S.E., and the *p* value is calculated by two-tailed *t* test. *D* and *E*, cryo-sections of GPS2-BKO and wild-type littermates spleens stained with H&E alone (*D*) or with metallophilic macrophage-specific antibody MOMA-1 (*E*). *White arrows* indicate cells positive for MOMA-1 after peroxidase detection.

T1 to T2 to T3 cells in GPS2-BKO mice (Fig. 3*B*). However, as predicted based on the RNA-Seq analysis (Fig. 1*I*), we observed almost a 3-fold reduction in the frequency of MZ B cells ($B220^+CD19^+IgM^{hi}CD21^{hi}CD23^{low}$) in the spleen of GPS2-BKO mice compared with wild-type littermates (Fig. 3*C*). On the contrary, the frequency of FO B cells ($B220^+CD19^+CD21^{low}CD23^{hi}$) shows a reciprocal increase in GPS2-BKO mice, indicating a switch between the two cell types in GPS2 mutant mice (Fig.

FIGURE 2. **Defective B cell development in the bone marrow (BM) of GPS2-deficient mice.** *A*, cell yield obtained from bone marrow preparation. *White bars*, WT; *black bars*, GPS2-BKO ($n = 7$). Bar graphs are ±S.E., and the *p* value is calculated by two-tailed *t* test. *B*, flow cytometry analysis and gating strategy. Representative plots are shown. Cells were pregated on a light scatter plot based on their size and granularity, doublets excluded on SSC-H *versus* SSC-W (side scatter height *versus* width) and FSC-H *versus* FSC-W (forward scatter height *versus* width) basis, dead cells excluded based on live-dead dye staining, and CD3+ and CD11b+ cells excluded before plotting the remaining live single $CD3^-CD11b^-$ lymphocytes on the first plot of the gating sequence. *C* and *D*, B cell subpopulation comparisons. *White bars*, WT; *black bars*, GPS2-BKO ($n = 7$). Bar graphs are ± S.E., and the *p* value is calculated by two-tailed *t* test. *E* and *F*, GPS2 mRNA expression in BM B cells from GPS2-BKO and control littermates measured by RT-qPCR (*E*) and validation of putative GPS2 target genes (*F*) in BM from GPS2-BKO and control littermates by RT-qPCR. Bar graphs represents the sample mean of three independent experiments ± S.D. *G*, ChIP analysis to measure GPS2 occupancy on the promoters of putative target genes in B cells purified from BM of WT mice. *H*, ChIP for GPS2 and FOXO1 in B cells purified from BM of either WT or GPS2-BKO mice. For ChIPs, data are representative of three independent experiments. Bar graphs represents the sample mean of technical replicates ± S.D. *, $p < 0.05$; **, $p < 0.01$. *I*, Western blotting for P-AKT (Ser^{473}) and P-FOXO1 in splenic B cells. *J*, representative track of GPS2 binding to the proximal promoter of FOXO1 gene by ChIP-Seq in murine 3T3-L1 differentiated adipocytes (37). The same pattern is observed in undifferentiated 3T3-L1 and human 293T cells (33, 37).

3*C*). In addition, the population of precursor marginal zone B cells (T2MZ; $CD19^+IgM^{high}CD21^{high}CD23^{high}CD1d^+$) also appears increased in frequency in mutant mice, suggesting a developmental block at this stage (Fig. 3*C*). In agreement with the differences observed via flow cytometry analysis, H&E staining of spleen sections reveals that the spleen architecture is disrupted in GPS2-deficient mice compared with control littermates, with enlarged and not well defined follicular structures (Fig. 3*D*). Reduced thickness of the marginal zone and disrupted follicles architecture is also confirmed by staining for the MZ-specific macrophage marker CD169 (Moma-1) (Fig. 3*E*). These results together suggest that within the B-2 conventional B cell compartment, GPS2 is specifically required for the terminal differentiation of MZ B cells, in addition to B cell perturbations in the bone marrow.

Next, we assessed the B-1 cell population. This population was also predicted by RNA-Seq analysis to be reduced, and indeed the $CD19^+CD43^+B220^{low}$ B-1 pool was approximately three times smaller in frequency in the spleens of mutant mice than in their WT littermates (Fig. 4, *A* and *B*). Within this population, the observed decrease appears to be solely due to the drop in the percentages of B-1a cells (defined as $CD19^+CD43^+B220^{low}CD5^+CD23^-$), whereas B-1b cell populations ($CD19^+CD43^+B220^{low}CD5^-CD23^-$) were similar in frequencies between the two groups (Fig. 4*B*). Likewise, we found B-1a cells to be reduced in the bone marrow of GPS2-BKO mice (Fig. 4*C*). Because IL-10 production is a functional hallmark of B1 cells, we further confirmed this phenotyping by measuring splenocyte IL-10 production *in vitro*. Most of B-1a and more than a half of B-1b cells produced IL-10 upon stimulation, confirming their immunophenotype (Fig. 4*D*), with no difference in the proportion of $IL\text{-}10^+$ cells within the B-1a or B-1b populations (Fig. 4*E*). To complete our phenotypic analysis, we also analyzed the B cells circulating through the peritoneal cavity, where the B-1 population is highly enriched. Again total cell number was unaffected by GPS2 deletion (Fig. 4*F*), but we found a lower frequency of B-1a cells in the peritoneum of GPS2-BKO mice, similar to results from the spleen and the bone marrow (Fig. 4, G and *H*), whereas the B-1b portion of $CD19^+$ cells was simultaneously more than 2-fold higher (Fig. 4*H*). The B-2 (conventional B cells) fraction of the peritoneal cavity B cells was similar between the two genotypes.

Lastly, to confirm the objectiveness of the manual flow cytometry data analysis, we subjected our flow cytometry data set to the automated data analysis by SPADE (59). Automated clustering was performed on $CD19^+$ events in bone marrow, spleen, and peritoneal cavity based on the markers whose expression delineates B cell subsets in those tissues. Upon clustering, all B cell subsets were clearly separated and identified as such based on the levels of lineage marker expression, with quantitative differences in cell percentages closely following the ones identified by blinded manual gating (Fig. 4*I* and data not shown).

Together, these analyses confirmed that GPS2 deletion in the B cell lineage impairs the development of B cells in the bone marrow at the stage of pre-B cells, with a mild but significant reduction in the amount of Transitional B cells recirculating to the bone marrow. In addition, they revealed that GPS2-BKO mice are defective in splenic MZ B cells and B-1a B cell compartments known as innate-like B cells (ILB) in both the spleen and the peritoneal cavity.

GPS2 Restricts TLR Signaling through Inhibition of Ubc13 Activity—B-1 and MZ cells together are considered ILB, because of their ability to respond to thymus-independent antigens and produce large amounts of polyreactive antibodies. In normal mice, ILBs are the major source of natural antibodies at steady state, and following TLR stimulation, they increase their production of IgM and IL-10 (60). To confirm whether the reduced number of ILBs in GPS2-BKO mice corresponded to an altered titer of natural antibodies, we measured plasma levels of all major isotype classes in unchallenged mice using the Milliplex isotyping kit (Millipore). To our initial surprise, GPS2-KO mice showed a significant increase rather than a decrease, in IgM levels, in addition to a mild but significant increase in IgG1 and IgG2b (Fig. 5*A*). IgG2a and IgG3 also trended to increase (Fig. 5*A*). At the same time, we found a corresponding increase of surface IgM expression per cell on multiple B cell subsets in GPS2-BKO mice (Fig. 5*B*). Because B-1 are the major producers of natural IgM, together with MZ cells, the significant increase in basal levels of IgM indicated that the secretory ability of the reduced pool of ILB cells was substantially increased, thus suggesting that IgM-producing cells might be constitutively activated in GPS2-BKO mice. This hypothesis was in accord with our previous work identifying GPS2 as a negative regulator of the TNFR1 signaling pathway and potentially other pro-inflammatory pathways (33). Thus, we asked whether constitutive activation of TLR signaling was observed in splenic B cells from GPS2-BKO mice by measuring the activation of intracellular mediators of TLR signaling. As shown in Fig. 5*C*, constitutive activation of critical steps of the signaling cascade downstream of TLR receptor was indeed observed upon GPS2 depletion, including a significant increase in both basal and inducible IκB degradation and p38, JNK, and IKKβ phosphorylation. In accord with the prediction of constitutively active NF κB signaling, sustained basal activation of a number of NFκB target genes, including TNFα, iNOS, MCP1, IL6, and LTA, was also observed in GPS2-deficient resting B cells (Fig. 5*D*). Notably, the up-regulation observed in absence of TLR stimulation is quite small in term of fold changes, despite being significant, possibly explaining the lack of enrichment in GO terms associated with inflammation among the DE genes defined by RNA-Seq in unstimulated B cells. To further confirm increased activation of a functional pro-inflammatory transcriptional program in absence of GPS2, we then compared the activation of known TLRs target genes in response to different ligands upon GPS2 deletion/overexpression. To this end, we used the following ligands: synthetic triacylated lipopeptide Pam3CSK4 (Pam3) to activate TLR1/2, bacterial LPS to activate TLR4, imidazoquinoline compound gardiquimod (Gardi) to activate TLR7, and CpG oligodeoxynucleotides (ODN 2395) to activate TLR9, and we measured the expression of known TLR target genes. First, we analyzed splenic B cells isolated from wild-type and GPS2-BKO littermates. In the presence of TLR4, TLR7, and TLR9 stimulation, the activation of TLR target genes *ccl3*, *ccl4*, and *IL6* is significantly increased in absence of GPS2 (Fig. 5*E*). The *GPS2* gene itself was down-regulated upon TLR7

stimulation, similar to what previously observed upon TNFR activation (33). Next, we measured the activation of representative TLR target genes in bone marrow-derived macrophages from wild-type and GPS2 overexpressing transgenic mice (aP2-GPS2) (33). As shown in Fig. 5*F*, GPS2 overexpression inhibits the activation of target genes *TNFα* and *CD14* (61–64) under most conditions, also in agreement with GPS2 overexpression in macrophages inhibiting the activation of pro-in-

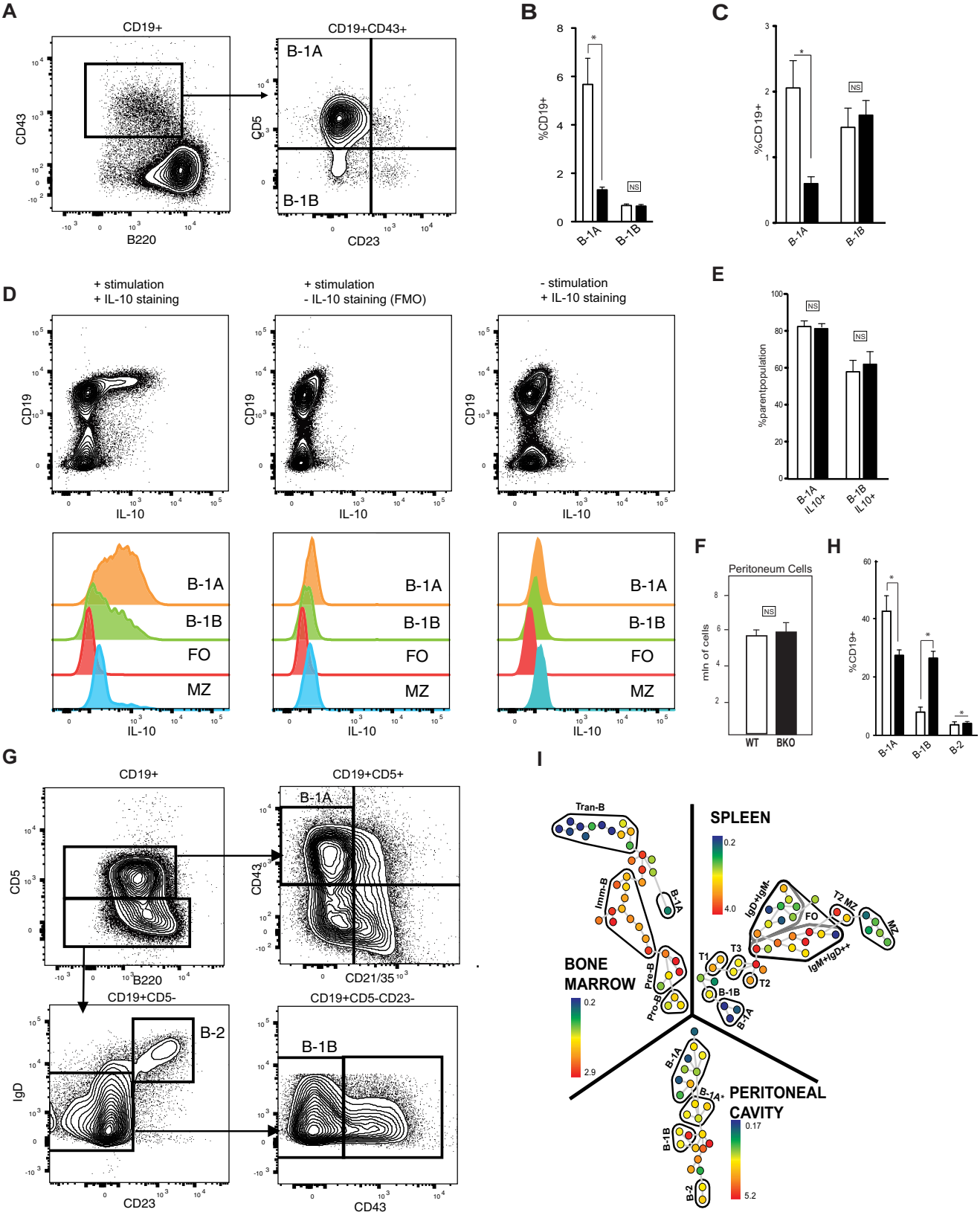

flammatory genes upon TLR4 stimulation by LPS (33). Thus, our results indicate that GPS2 is required for restricting signal transduction downstream of multiple TLR receptors.

We previously showed that GPS2-mediated regulation of TNFR1 is achieved through inhibition of TRAF2/Ubc13 activity. Because of the similarities between the TNFR1 and TLR signaling pathways in terms of usage of non-proteolytic Lys^{63} ubiquitin signaling for signal transduction, we hypothesized that GPS2 inhibitory role toward TLR signaling was mediated by a similar mechanism. In support of this hypothesis, we observed that GPS2 overexpression caused a significant decrease in the amount of LPS-induced autoubiquitination, and therefore activation, of TRAF6, the E3 ligase that partner with Ubc13 in the TLR signaling pathway (Fig. 6*A*). Conversely, increased TRAF6 autoubiquitination and increased levels of Lys^{63} ubiquitin chains associated with TLR7 were detected in GPS2-deficient B cells (Fig. 6*B*). Again, ubiquitination was not further increased upon LPS treatment, indicating that removal of the inhibitor is sufficient for unleashing the activation of the ubiquitin machinery even in the absence of ligand stimulation.

These results, combined with our recent report of GPS2 playing an important role in controlling lipid metabolism through inhibition RNF8/Ubc13 activity in the nucleus and stabilization of the histone methyltransferase JMJD2/KDM4A, suggested that distinct GPS2 functions within different cellular compartments similarly depend on the inhibition of Ubc13-containing complexes (37). Based on our previous data indicating that GPS2 can directly interact not only with each of the specific E3 ligases present in the complexes we investigated (namely TRAF2, TRAF6, or RNF8) but also with Ubc13 itself (33, 37), we asked whether GPS2 could directly inhibit the enzymatic activity of the E2-conjugating enzyme rather than modulating a number of different ligases. To address this question, we performed an *in vitro* ubiquitination assay to assess the ability of the Ubc13/Uev1A E2-conjugating enzyme complex to form ubiquitin chains in the presence or absence of bacterially purified recombinant His-GPS2. As shown in Fig. 6*C*, the direct synthesis of ubiquitin chains by the Ubc13/Uev1A complex is impaired in presence of GPS2, thus confirming that GPS2 inhibitory action does not require the presence of an E3 ligase. In particular, GPS2 significantly inhibits the elongation of ubiquitin chains, whereas neither the formation of di-ubiquitin short chains nor the charging of avidin-tagged or FLAG-tagged ubiquitin onto Ubc13 is affected by GPS2 (Fig. 6, *C* and *D*).

Together, these results suggest that GPS2 inhibitory activity within different signaling complexes depends on GPS2 directly inhibiting the enzymatic activity of Ubc13 to prevent the synthesis of extended Lys^{63} ubiquitin chains. To confirm this hypothesis in the context of pro-inflammatory signaling pathways, we used a chemical inhibitor called NSC697923 to inhibit Ubc13. NSC697923 was previously validated in a model of diffuse large B cell lymphoma in which it was able to suppress constitutive NF-κB activation and cell proliferation/survival (65). As shown in Fig. 6 (*E* and *F*), both the hyperactivation of p38 and JNK, as well as the increased expression of pro-inflammatory target genes in GPS2-BKO cells, were rescued by NSC697923. These results confirm that Ubc13 hyperactivation is responsible for the phenotype observed in GPS2-deficient splenic B cells and suggest that Ubc13 unrestricted activation in absence of GPS2 underlies the misregulation of multiple signaling pathways in GPS2-BKO mice. Intriguingly, the most up-regulated gene in GPS2-null B cells is the HECT E3 ligase NEDD4 (supplementalTableS1 and Fig. 6*G*). HECT ligases promote ubiquitination through direct substrate ubiquitination rather than through E2-mediated synthesis of ubiquitin chains, and NEDD4, in particular, appears to have a preference for the synthesis of Lys^{63} ubiquitin chains (66–68). Thus, we are tempted to speculate that NEDD4 up-regulation might reflect an attempt at compensating for the misregulation of Ubc13-mediated Lys^{63} ubiquitination events.

Inhibition of BCR Signaling by GPS2 Is Required for Notch-mediated Differentiation of MZ Cells—In B cells, TLR and BCR signaling pathways present extensive cross-talk, including both TLR-mediated sensitization of BCR activation, as well as common regulatory strategies and shared signaling mediators. Among them, the use of Ubc13-dependent ubiquitination is a key signaling mechanism downstream of multiple receptors involved in immune responses (1, 31). Thus, based on GPS2 ability to inhibit Ubc13 activity *in vitro*, we asked whether its inhibitory role extended to BCR activation. Upon stimulation of splenic B cells with IgM, we observed a strong increase in both basal and inducible phosphorylation of p38 in B cells isolated from GPS2-BKO compared with WT littermates, suggesting that GPS2 is required for restricting signal transduction downstream of both BCR and TLR receptors (Fig. 7*A*). A smaller, but consistent, increase in JNK activation was observed only in basal conditions, whereas ERK phosphorylation upon IgM stimulation was slightly decreased (Fig. 7*A*). To confirm that the increase in p38 activation is caused by GPS2-mediated inhibition of ubiquitination, we asked whether activation of

FIGURE 4. **Reduced B-1 B cell population in GPS2-BKO mice.** *A*, flow cytometry analysis of splenic B-1 populations. Representative plots are shown, and the cells are pregated as described above. *B*, splenic B-1 populations comparison. *White bars*, WT; *black bars*, GPS2-BKO ($n = 7$). Bar graphs are ± S.E., and the *p* value is calculated by two-tailed *t* test. *C*, flow cytometry showing B1-A and B1-B cell population in the bone marrow. *White bars*, WT; *black bars*, GPS2-KO ($n = 4$). *D*, IL-10 production by splenic B cells. Representative plots are shown for stimulated fully stained cells, stimulated fluorescence minus one control (no IL-10 antibody added), and non-stimulated fully stained cells. All cells were incubated with monensin. IL-10 production by different B cell subtypes is shown in histograms in the *bottom row* of plots. *E*, indirect quantification of IL-10+ B cell percentage by mean fluorescence intensity. *White bars*, WT; *black bars*, GPS2-BKO ($n = 3$). *F*, cell yield obtained from peritoneal cavity lavage. *G*, flow cytometry analysis of peritoneal cavity B-1 populations. Representative plots are shown, and the cells are pregated as described above. *H*, peritoneal cavity B-1 populations comparison. *White bars*, WT; *black bars*, GPS2-BKO ($n = 7$). *I*, automatic clustering representation of the cytometry data set. Unsupervised SPADE clustering into 30–40 nodes/tree was performed using CD1d/5/21/23/43/93/45RO/IgD/IgM lineage marker channels, and the nodes were annotated based on the known expression of lineage markers in various B cell subsets. A representative GPS2-BKO sample is shown. Fold increase of GPS2-BKO node percentages over averaged WT is shown as color.

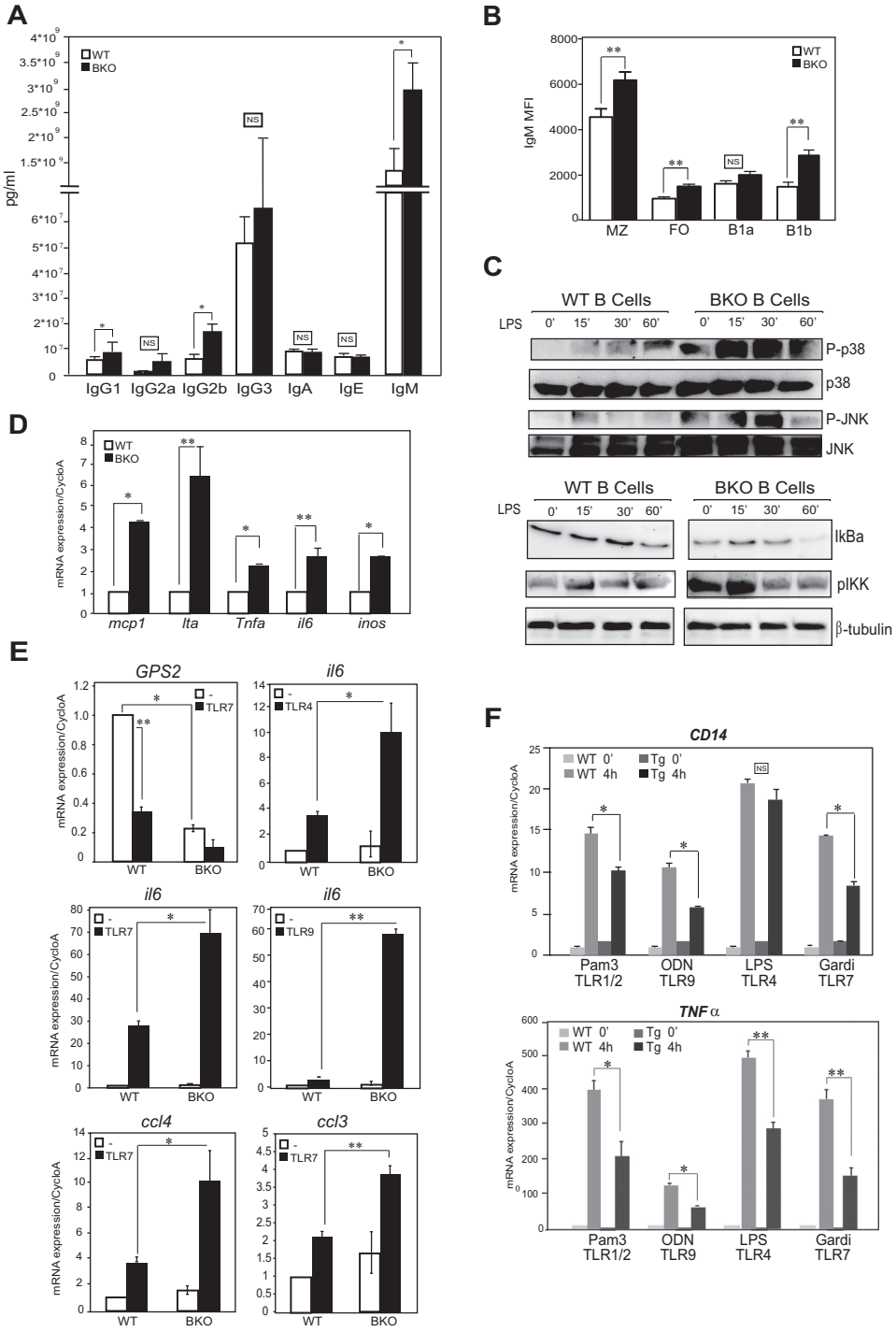

FIGURE 5. **GPS2 deletion promotes hyperactivation of TLR signaling.** *A*, immunoglobulin profiling of IgG1, IgG2a, IgG3, IgA, IgE, and IgM is performed on plasma from unchallenged WT and GPS2-KO mice using the Procarta mouse Ab isotyping 7-Plex kit ($n = 4$). *B*, IgM expression on cell surface of WT and GPS2-KO MZ, FO, B1-a, and B1-b cell. *White bars*, WT; *black bars*, GPS2 BKO ($n = 7$). *C*, Western blotting for P-p38, p38, P-JNK, and JNK (*top panel*) and IKBα and phospho-IKK (*bottom panel*) upon LPS treatment of splenic B cells from WT and GPS2-BKO mice. On the *right* is shown quantification of the blots by volume densitometry. Normalization was done against the unphosphorylated protein when possible or using tubulin as a loading control. Fold changes are calculated toward the normalized level of each protein at time 0. *D*, RT-qPCR analysis of TLRs target genes in unstimulated B cells from GPS2-BKO and control littermates. *E*, RT-qPCR analysis of TLRs target genes upon stimulation with Gardi, ODN, or LPS. Bar graphs represent the sample mean of three independent experiments ± S.D. *, $p < 0.05$; **, $p < 0.01$. *F*, gene expression analysis by RT-qPCR performed on RNA from wild-type GPS2-overexpressing macrophages (33) (Ap2-GPS2 transgenic mice) upon treatment with indicated ligands. The data are representative of three independent experiments. Bar graphs represents the sample mean of technical replicates ± S.D. *, $p < 0.05$; **, $p < 0.01$.

Ubc13/TRAF6-dependent ubiquitin signaling downstream of BCR receptor activation is affected by the lack of GPS2. As shown in Fig. 7*B*, autoubiquitination of TRAF6 was indeed higher in GPS2-deficient B cells rather than WT splenic B cells stimulated with IgM. Together, our data confirm that GPS2-mediated inhibition of Lys^{63} ubiquitination plays a significant role in modulating the activation of both BCR and TLR signaling in B cells.

Intriguingly, the strength of BCR signaling has been shown to play a critical role in the cell fate decision between FO and MZ cell types in the spleen. In particular, weak BCR signaling was associated with MZ B cell development, whereas a strong BCR signaling is thought to facilitate the commitment toward the FO B cell lineage via inhibition of Notch2 signaling (69–72). Accordingly, Notch2 haploinsufficiency leads to a marked reduction in both MZ and B1 B cells (73). Based on Notch2

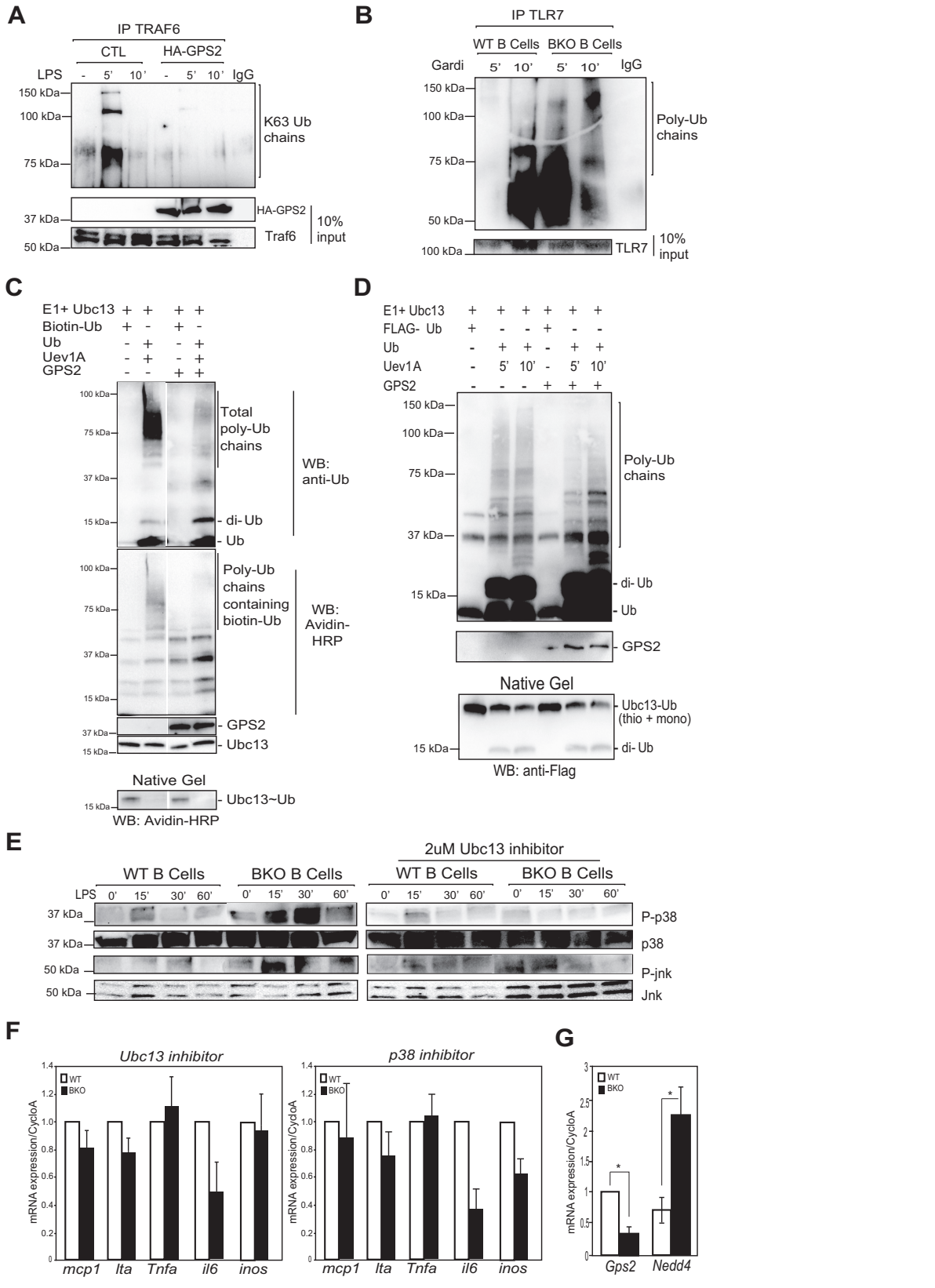

target gene Deltex (*Dtx1*) being the second most significantly down-regulated gene after GPS2 in GPS2-BKO cells (supplemental Table S1), we hypothesized that aberrant activation of the BCR pathway and thus inhibition of Notch2 signaling could be the underlying mechanism of the reduced MZ phenotype in GPS2-BKO mice. In support of this hypothesis, we confirmed that not only *Dtx1*, but also other Notch2 target genes, such as *Hes1* (*Hairy enhancer of split 1*) and *Hes5* (*Hairy enhancer of split 5*), were down-regulated in splenic B cells from GPS2-BKO whereas the expression of Notch2 receptor itself was unchanged (Fig. 7*C*). Notably, the defect in gene expression was dependent on both p38 and Ubc13 activation because gene down-regulation was rescued by inhibiting either p38 or Ubc13 activity (Fig. 7*C*). Also, the down-regulation was specific to sorted MZ cells and not observed in the corresponding FO population (Fig. 7*D*). Thus, our results suggest that GPS2 requirement for MZ B cell differentiation in the spleen is likely tied to the regulation of BCR signaling, with GPS2 deletion causing exacerbated activation of BCR and therefore indirectly affecting the activation of important Notch2-dependent cell fate commitment genes.

Overall, we conclude that GPS2 plays a broad inhibitory effect over the activation of different signaling pathways via modulation of Ubc13 enzymatic activity (Fig. 7*E*). In particular, our findings indicate that the presence of GPS2 in murine B cells is essential for restricting the activation of the PI3K/AKT and TLR/BCR pathways. Conversely, loss of GPS2 leads to multiple defects during B cell development because of aberrant activation of Lys^{63} ubiquitination events and altered gene expression programs downstream of the misregulated signaling pathways.

Discussion

Stringent regulation of pro-inflammatory pathways is critical to allow for a rapid and effective response to infections and other external injuries while preventing the aberrant and damaging activation of autoimmune reactions and other forms of chronic inflammation. Non-proteolytic ubiquitination mediated by the E2-conjugating enzyme Ubc13 represents a critical component of multiple pro-inflammatory signaling pathways converging on the activation of the transcription factor NF-κB. Accordingly, it is an important regulatory step that can be negatively controlled by endogenous inhibitors of NF-κB activation, such as the deubiquitinases A20, CYLD, and MYSM1 (21, 23, 74, 75). In this manuscript, we characterize GPS2 as a novel, important negative regulator of non-proteolytic ubiquitination that acts directly on Ubc13 and inhibits the formation of extended Lys^{63} ubiquitin chains synthetized by the Ubc13/Uev1A complex. Mechanistically, our initial *in vitro* characterization of GPS2 inhibitory activity suggests possible similarities to the mechanism of action of another Ubc13 inhibitor that is critical for the regulation of DNA damage response, the deubiquitinating enzyme OTUB1 (76–78). However, more detailed structural studies will be required to fully elucidate the mechanistic details of GPS2 inhibition toward the Ubc13 complex.

The identification of GPS2 as an endogenous inhibitor of Ubc13 activity has critical implications not only for immune response pathways but also for other key cellular processes relying on Lys^{63} ubiquitination events. Further studies will be required for addressing each case individually with consideration of the cross-talks among different ubiquitin machineries. However, the initial observations presented here, together with previous reports, seem to confirm that GPS2-mediated inhibition of Lys^{63} ubiquitination is functionally critical for a number of pathways that utilize Ubc13, including TNFR1, TLR, BCR, and PI3K/AKT signaling pathways.

In the context of pro-inflammatory responses, here we have elucidated, in overexpressing macrophages and GPS2-deficient B cells, the role of GPS2 in the response to a number of TLR ligands. Overall, our data confirm GPS2 critical role in preventing the constitutive, basal activation of the signaling cascade that links liganded TLR receptors to the transcriptional regulation of NF-κB target genes. These results are consistent with studies published during the compilation of this manuscript reporting that GPS2 depletion in macrophages promotes a pro-inflammatory gene signature corresponding to enhanced TLR signaling (38). Intriguingly, our results indicate that the extent of the changes in gene expression associated with GPS2 reduction/deletion is likely reflective of broad effects on the pro-inflammatory signaling cascades rather than being limited to a sole transcriptional role for GPS2 as part of the NCoR/SMRT corepressor complexes.

Constitutive activation of NF-κB signaling is widely reported as a pro-survival strategy in cancer, and the transduction pathways upstream of NF-κB nuclear translocation are affected in a large number of hematological malignancies (29, 79–82). In particular, somatic mutations leading to constitutive NF-κB activation have been identified in negative regulators of non-proteolytic Lys^{63} ubiquitination events, such as the deubiquitinases and tumor suppressors CYLD and A20 (26, 30). Constitutive activation of the NF-κB pathway is also a component of the oncogenic program promoted by viral proteins, such as the human T cell leukemia virus (HTLV-1) activator Tax (83), that promote GPS2 down-regulation upon viral infection (84, 85). Because recent work indicates that Tax-induced NF-κB activation depends on viral hijacking of the endogenous RNF8 and Ubc13 enzymes to promote Lys^{63} ubiquitination (86), we are tempted to speculate that removal of GPS2-mediated inhibi-

FIGURE 6. **GPS2 restricts TLR signaling through inhibition of Ubc13 activity.** *A*, TRAF6 autoubiquitination upon LPS stimulation is measured by IP-WB using an antibody specific for Lys^{63}-linked Ub chains after 24 h of transient HA-GPS2 overexpression in 293T cells. *CTL*, control. *B*, IP-WB using anti-TLR7 and total Ub antibody in B cell from WT and GPS2-KO B cells stimulated with Gardi. *C*, *in vitro* ubiquitination assay performed in the presence or absence of recombinant His-GPS2. E1 and Ubc13 are initially loaded with biotin-labeled ubiquitin ± GPS2. Then Uev1A is added, and excess unlabeled ubiquitin and nascent ubiquitin chains are monitored after 5 min at 37 °C by Western blotting for ubiquitin or avidin-HRP. Loading and unloading of ubiquitin from Ubc13 (thioester bond) is measured via avidin-HRP WB under native conditions. *D*, *in vitro* ubiquitination assay using FLAG-Ub to preload Ubc13 prior to Uev1a addition. *E*, Western blotting analysis of LPS induced activation of p38 and JNK showing that inhibition of Ubc13 activity by the small molecule NSC697923 is sufficient to rescue for the lack of GPS2. *F*, both Ubc13 inhibition by NSC697923 and p38 inhibition by SB203580 rescue the basal activation of pro-inflammatory target genes (Fig. 5*D*). *G*, expression of *Nedd4* by RT-qPCR in splenic B cells.

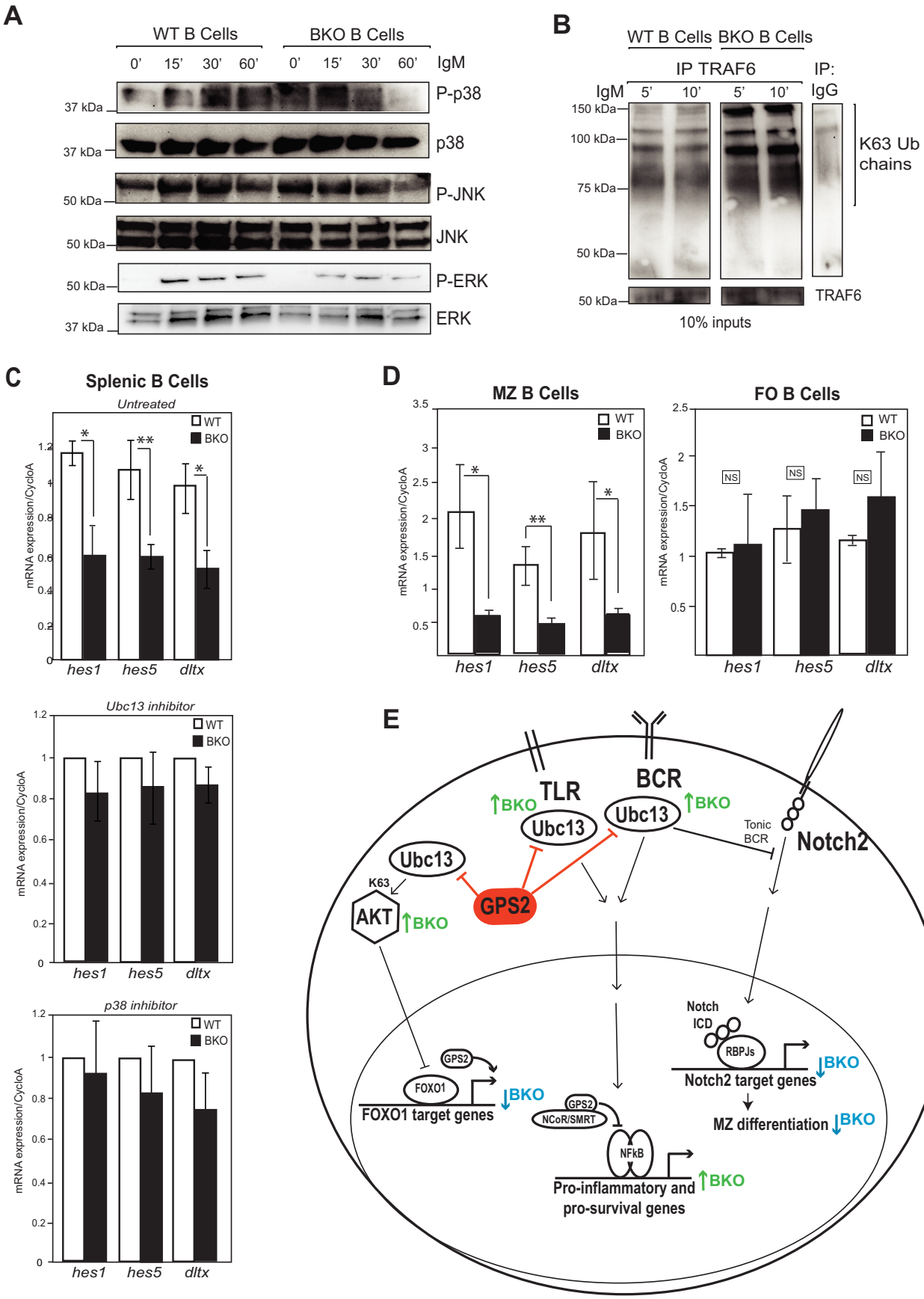

tion of Ubc13 activity might be a critical component of the viral strategy for controlling the growth and survival of HTLV-infected cells. These observations together raise the intriguing possibility that GPS2 itself could serve a tumor suppressive role in cells where the aberrant constitutive activation of NF-κB signaling contributes to tumor development and progression. This hypothesis is in agreement with recent reports of GPS2 being mutated or deleted in different tumor types (47, 87–94), thus providing the rationale for further dedicated studies to assess the role of GPS2 in cancer.

Understandably, the proper integration of signals coming from multiple receptors that share Ubc13 as an important signaling mediator, including BCR, TLR, BAFF, and CD40, is critical for a number of functions, including the maturation and homeostasis of B cells, as well as their ability to mount proper immune responses. Although this study has focused on the role played by GPS2 during mouse B cell development, further studies will be required to investigate to what extent GPS2-deficient mice can respond to infections and injuries through normal innate and adaptive immune responses and whether the lack of GPS2 affects the development of autoimmune diseases.

Here, the phenotypical characterization of the normal development of GPS2-BKO mice has revealed a broad role for GPS2 in early and late B cell developmental stages, with the conditional deletion of GPS2 in the B cell lineage leading to a mild accumulation of pre-B cell in the bone marrow and a significant decrease in splenic MZ and B-1 cells. Intriguingly, our data support a model in which both phenotypes are related to the loss of GPS2-mediated regulation of Ubc13 activity. Unrestricted activation of AKT in the earliest stages of B cell development, prior to mature BCR expression, appear to alter the activation of a FOXO1-dependent transcriptional gene network that is required for immunoglobulin chain recombination and receptor editing. Later defects are instead associated with the hyperactivation of pathways regulated by Ubc13-mediated Lys^{63} ubiquitination leading to constitutive activation of BCR signaling, preventing Notch2-mediated cell fate decision events. Notably, in both instances the same target genes that are downstream targets of the pathways that are regulated by GPS2 in a non-genomic fashion through inhibition of Ubc13 activity are also directly regulated by GPS2 as a transcriptional cofactor. Thus, our results together support a comprehensive model in which the genomic and non-genomic actions of GPS2 in the cell are exquisitely coordinated.

To our initial surprise, the GPS2-BKO mice phenotype in regard to B1 and MZ cells is very similar to that of mice deleted of Ubc13 itself (95). However, similar defects are observed in mouse knock-out models of both activators and inhibitors of BCR/TLR signaling (96) (*i.e.* TAB2/3, A20, IκBNS, TRAF6, TAB2/3, and MALT1) (26, 97–100). We speculate that these apparent discrepancies are indicative of the fact that having constitutive or exacerbated signaling, at least during particular stages of development, can be as damaging as having a reduced or impaired response, thus supporting the importance of endogenous regulators, such as GPS2, to maintain tight regulation in both directions.

Lastly, it is noteworthy that naïve GPS2-BKO mice present increased plasma levels of natural antibodies, particularly IgM, despite the lower number of innate-like B cells. This is consistent with higher level of serum Igs observed in other models of BCR/TLR hyperactivation (26, 100–102), whereas the production of natural antibodies is usually impaired upon deletion of key mediators of both pathways (96, 99, 103). Thus, the increase in natural antibody production *in vivo* is in accord with the constitutive activation of TLR/BCR signaling observed in GPS2-null B cells. This suggests that the reduced number of innate-like B cells in GPS2-BKO mice might be functionally compensated by their enhanced activation. In addition, secreted IgM would further enhance BCR signaling while restricting the size of the B1 and MZ compartments, thus possibly establishing a forward feedback loop that influences B cell survival and homeostasis at steady state (104, 105).

In conclusion, the characterization of GPS2 B cell-specific conditional knock-out mice has confirmed *in vivo* the important role played by GPS2 in the regulation of Ubc13 enzymatic activity within multiple signaling pathways and revealed a comprehensive view of how the coordinated regulation of non-proteolytic ubiquitination in different signaling pathways converges in mediating key developmental steps during B cell development.

Experimental Procedures

Mice—aP2-GPS2-overexpressing mice were previously described (33). Conditional $Gps2^{flox/flox}$ mice were generated by inGenious Targeting Laboratory. The 9.52-kb region used to construct the targeting vector was first subcloned from a positively identified C57BL/6 (RP23: 91G16) BAC clone into a ~2.4-kb backbone vector (pSP72, Promega) containing an ampicillin selection cassette. The total size of the targeting construct (including vector backbone and Neo cassette) is ~13.62 kb. The region was designed such that the short homology arm extends ~2.55 kb 3′ to exon 6. The long homology arm ends 5′

FIGURE 7. **Inhibition of BCR signaling by GPS2 is required for Notch mediated differentiation of MZ cells.** *A*, immunoblot analysis of MAPK kinases p38, JNK, and ERK activation upon BCR stimulation with 10 μg/ml IgM for the indicated times. On the *right* is shown quantification of the blots by volume densitometry. Normalization was done against the unphosphorylated protein. Fold changes are calculated toward the normalized level of each protein at time 0. *B*, TRAF6 autoubiquitination upon IgM stimulation of splenic B cells from wild-type and GPS2-BKO mice measured by IP-WB using an antibody specific for Lys^{63} ubiquitin chains. *C*, expression of Notch2 target genes *Hes1*, *Hes5*, and *Deltex* by RT-qPCR in splenic B cells from wild-type and GPS2-BKO mice. The reduced expression observed in GPS2-BKO cells is similarly rescued by inhibiting Ubc13 or p38 activity. *D*, expression of Notch2 target genes *Hes1*, *Hes5*, and *Deltex* by RT-qPCR in marginal zone and follicular zone B cells sorted from splenocytes of WT and GPS2-BKO mice. Bar graphs represents the sample mean of three independent experiments ± S.D. *, $p < 0.05$; **, $p < 0.01$. *E*, graphical summary. GPS2 mediated regulation of TLR, BCR, and AKT signaling pathways is achieved through inhibition of Ubc13 enzymatic activity. B cell-specific deletion of GPS2 results in decreased expression of FOXO1-dependent genes that are required for Ig recombination and defective development of bone marrow B cells at the pre-B cells stage. GPS2 is also required at later stages of development to prevent the constitutive activation of BCR and TLR signaling pathways and restrict the production of natural antibodies. Strong BCR is not permissive for Notch2 signaling and leads to reduced differentiation of MZ B cells.

to exon 3 and is 6.07 kb long. A pGK-gb2 loxP/FRT Neo cassette is inserted on the 3′ side of exon 6, and the single loxP site is inserted 5′ of exon 3. The target region is 0.90 kb and includes exon 3–6. The targeting vector was linearized by NotI and then transfected by electroporation of BA1 (C57BL/6 × 129/SvEv) hybrid embryonic stem cells. After selection with G418 antibiotic, surviving clones were expanded for PCR analysis to identify recombinant ES clones and control for retention of the third LoxP site. Secondary confirmation of positive clones was performed by Southern blotting analysis prior to microinjection into C57BL/6 blastocysts. The resulting chimeras with a high percentage agouti coat color were mated to wild-type C57BL/6 mice to generate F1 heterozygous offspring. The Neo cassette was excised by crossing with FLP mice (The Jackson Laboratory) to generate F2 heterozygous mice with Neo deletion in somatic cells and F3 heterozygous mice with Neo deletion in germ cells. Homozygous $Gps2^{flox/flox}$ mice were then used for crossing with heterozygous 129sv CD19-Cre mice (48) (The Jackson Laboratory). The CD19 promoter specifically directs expression at the earliest stages and throughout B-lymphocyte development and differentiation (48). Because the Cre cassette is inserted into exon 2 of CD19 gene, functionally disrupting the gene, homozygous CD19-Cre mice are CD19-deficient. However, heterozygous mice are phenotypically normal and can be used for specific deletion of floxed targets in B-lymphocytes (48). Wild-type mice used as control for all analyses presented here were littermates $Gps2^{flox/flox}$/$CD19Cre^{-}$. All experiments are done with mice 10–16 weeks old.

Flow Cytometry Analysis and Sorting—Bone marrow cells were flushed from femoral bone by flush, peritoneal cavity cells were isolated by lavage of the peritoneal cavity, and splenic B cells were isolated from single cells suspension of total splenocytes prepared according to standard protocols (106). B cell purification was achieved by magnetic depletion using the MACS Pan B cells isolation kit (Miltenyi Biotech). Purity of the B cell populations was verified by flow cytometric analysis with CD19, CD11b, and CD3 labeling. Flow cytometry analyses were performed using the following anti-mouse Abs: BV510 anti-B220, FITC anti-CD3, PE anti-CD23, PE-594Dazzle anti-IgM, APC anti-CD19, PerCPCy5.5 anti-CD21, PE Cy7 anti-CD5 (Biolegend); BV395 anti-IgD, BV421 anti-CD1d, BV650 anti-AA4.1, BUV737 anti-CD43, FITC anti-IL-10, BV496 anti-CD3 (BD Biosciences), and A700 anti-CD11b (Ebioscience). Single cell suspensions were stained with NIR Zombie dye, washed, preblocked with mouse FcBlock (Biolegend), and stained with antibody cocktails in the presence of Brilliant Violet buffer (BD Biosciences). Ultracomp beads (eBioscience) stained with abovementioned antibodies and ArC beads (Life Technologies) stained with NIR Zombie dye were used for compensation in FACSDIVA. All data were acquired on a FACSARIA II SORP (BD Biosciences). To minimize fluorescence data variability, Ultra Rainbow Beads (Spherotech) were used for target value tracking. At least 200,000 events were collected from each sample. At least 96% purity was confirmed for all sorted populations.

Flow Cytometry Data Analysis—All manual analysis was performed by a blinded investigator using FlowJo 10, and statistical analysis was performed with GraphPad Prism 5. For SPADE automated clustering, automatically compensated data were imported into Cytobank, and all consequent analysis was performed within Cytobank platform (107) Live, single-particle, $CD3^{-}CD11b^{-}CD19^{+}$ events were extracted and analyzed; events were down-sampled at 80% clustered into 30–40 nodes/tree using CD1d, CD5, CD21, CD23, CD43, CD93, B220, IgD, and IgM as clustering channels. Trees were annotated based on the known expression of signature markers.

Cell Culture and Treatments—B cells purified from spleen of $Gps2^{-/-}$ and wild-type littermates were cultured at 10^6 cells/ml in RPMI 10% FBS, 100× penicillin/streptomycin, and treated with 1 μg/ml LPS (TLR4 ligand), 1 μM of ODN 2395 (TLR9 ligand), or 1 μg/ml gardiquimod (TLR7 ligand) (Invivogen) for 4 h. Treatment with 10 μg/ml of purified rat anti-mouse IgM (BD Pharmingen) was performed in the same culture condition for different time courses. For IL-10 stimulation and phenotyping, spleen cells were stimulated for 5 h in the presence of 10 μg/ml LPS, 50 ng/ml phorbol 12-myristate 13-acetate, and 500 ng/ml ionomycin in presence of 2 μM monensin as described previously (108) stained for surface markers, fixed with IC fixation buffer (Biolegend), permeabilized with IC permeabilization/wash buffer (Biolegend), and stained for IL-10. 293T cells were cultured in 4.5 g DMEM/liter glucose, 10% FBS, and 100× penicillin/streptomycin. For cell transfection, Lipofectamine 2000 was used following the manufacturer's protocol (Life Technologies). After 24 h, the cells were treated 1 μg/ml LPS for 5 or 10 min, lysated, and then subjected to IP/WB. Bone marrow-derived macrophages were isolated as differentiated *in vitro* as previously described (33). For gene expression analysis they were treated with 10 μg/ml lipopeptide Pam3CSK4 (Pam3) TLR1/2 activator, 1 μg/ml LPS TLR4 activator, 10 μg/ml imidazoquinoline compound Gardi TLR7 activator, or 1 μM CpG oligodeoxynucleotides (ODN 2395) TLR9 agonist for 4 h. In rescue experiments cells were treated for 4 h with chemical inhibitors at the following concentrations: NSC697923 2 μM (Sigma-Aldrich, Ubc13 inhibitor), SB203580 25 μM (Invivogen, p38 MAPK inhibitor).

H&E and Immunohistochemistry Staining of Splenic Sections—Cryosections from Gps2-BKO mice and wild-type littermates were prepared at 10-μm thickness, fixed in 10% formalin solution, and stained with hemoatoxilin solution (Fisherbrand) and eosin solution (Fisherbrand) according to standard protocols. For immunohistochemistry, sections were blocked with 10% donkey serum, 1% BSA and then stained with primary antibody overnight at 4 °C and secondary antibody for 1 h at room temperature. The antibodies used are rat anti-mouse MOMA-1 (AbD Serotec-Bio-Rad) and HRP-conjugated anti-RAT (Cell Signaling). The reaction was developed using the DAB liquid substrate dropper system (Sigma) following the manufacturer instructions.

Western Blotting and Abs—Whole cell lysates were prepared in radioimmune precipitation assay buffer, and protein extracts were resolved by SDS-PAGE and then electrotransferred onto PVDF membrane. The following Abs were used: anti-GPS2 was generated in rabbit against a peptide representing amino acids 307–327 (33); anti-Ubc13 (YD-16), anti-JNK1/2 (FL), anti-TRAF6 (H-274), anti-EKR (K23) (Santa Cruz Biotechnology);

anti-phospho JNK (4668), anti-phospho p38 (4511S), anti-IkBa (9247), anti-p38 (9212), and anti-phospho ERK1/2 (E10) (Cell Signaling); mouse anti-B-tubulin (Sigma); mouse anti-HA (Upstate Biotechnology); and anti-polyubiquitin-Lys^{63} linkage-specific (Enzo Life Science).

In Vitro Ubiquitination and Protein Purification—Ubiquitination assays were carried out at 37 °C in 50 mM Tris-HCl, pH 7.6, 50 mM NaCl, 5 mM $MgCl_2$, 5 mM ATP, 1× ubiquitin aldheide, and 2 mM DTT. GPS2 was produced as a His tag fusion protein in BL21 *Escherichia coli*, resin-purified on nickel-nitrilotriacetic acid beads, and eluted accordingly to manufacturer's protocol (Life Technologies). Purified recombinant enzymes and ubiquitin were purchased from Boston Biochem. The reaction was first assembled on ice with 50 nM recombinant E1, 1 μM Ubc13, 5 μg of tagged Ub (either Flag-tagged or biotin-tagged) with or without GPS2. Ubiquitination was then promoted by adding 1 μM Uev1A and unlabeled ubiquitin in excess (20 μg). The reactions were stopped after 5 or 10 min at 37 °C by boiling in DTT-containing SDS loading buffer, and proteins were resolved by SDS-PAGE and immunoblotted. For native gels, DTT was excluded from the reaction, we used DTT-free SDS loading buffer, and samples were not boiled.

Chromatin Immunoprecipitation, RNA Extraction, RT-qPCR, and RNA-Seq—ChIP was performed as previously described (37). Total RNA was prepared with RNeasy® plus mini kit (Qiagen) according to the manufacturer's protocol. RNA was retrotranscribed into cDNA using iScript® reverse transcription supermix for RT-qPCR (Bio-Rad), and qPCR was performed using the Fast SYBR® Green Master Mix (Life Technologies) according to the manufacturer's protocol. All samples were run in triplicate using a ViiA7® qPCR machine (Appied Biosystem), and normalization was calculated to the housekeeping gene cyclophilin A. Significance of gene expression analyses was calculated by two-tailed, two-sample *t* test with unequal variance among replicate experiments as indicated in the figure legends. The sequences of oligonucleotides used for gene expression analysis are available upon request. For RNA-Seq experiments RNA quality was assessed on the Agilent 2100 Bioanalyzer (Boston University Medical Center Microarray Core). cDNA libraries were prepared either with the NEBNext ultra directional library preparation kit for Illumina or with the Illumina TruSeq stranded total RNA sample prep kit with rRNA depletion by RiboZero Gold and then sequenced on a HiSeq2500 (single-strand, 50-bp reads).

Bioinformatics Analysis of RNA-Seq Samples—The sequencing reads were aligned to the mouse genome mm8 by using bowtie (109), and the aligned sequencing reads were counted over gene exons by using HOMER that computed also the RPKM values. The differentially expressed genes between KO and WT samples were statistically defined by a two-tailed, two-sample *t* test between the replicates (p value $<$ 0.05). The heat maps of differential expressed genes were displayed by using R packages "pheatmap" and "gplots" (heatmap.2() functions). To characterize the differential use of V, D, and J segments, we have downloaded the sequences from IMGT database, and their expression levels were computed with RSEM (110). The RNAseq data are available on the GEO website under accession number GSE92751.

Author Contributions—C. L. designed and performed most of the experiments with the help of C. T. C., H. E. J., A. L., and S. P.; C. L. and A. B. designed and carried out all FACS analyses; M. C. was responsible for the *in vitro* characterization of GPS2-Ubc13 activity; S. M. and B. T. carried out the bioinformatic analysis of RNA-Seq data; and V. P. conceived the project, supervised the research team, and wrote the manuscript with the help of C. L., M. D. C., A. B., J. C., and B. S. N.

Acknowledgments—We are grateful to Drs. X. Varelas, T. Kepler, and G. Denis for insightful comments and discussions and to all members of the Varelas, Garcia-Marcos, Ritter, and Perissi labs for useful suggestions, comments, and technical advice during joint lab meetings. We thank Drs. F. Raval and J. Defuria for teaching us how to isolate and culture murine B cells and for their helpful suggestions in designing FACS experiments. All flow cytometry experiments were performed at the Flow Cytometry Core Facility at Boston University School of Medicine. RNA-Seq was performed with support from the Genomic Science Institute at Boston University and through the services of the Genomics Core at Tufts University.

References

1. Bhoj, V. G., and Chen, Z. J. (2009) Ubiquitylation in innate and adaptive immunity. *Nature* **458,** 430–437
2. Popovic, D., Vucic, D., and Dikic, I. (2014) Ubiquitination in disease pathogenesis and treatment. *Nat. Med.* **20,** 1242–1253
3. Malynn, B. A., and Ma, A. (2010) Ubiquitin makes its mark on immune regulation. *Immunity* **33,** 843–852
4. Stringer, D. K., and Piper, R. C. (2011) Terminating protein ubiquitination: hasta la vista, ubiquitin. *Cell Cycle* **10,** 3067–3071
5. Nagy, V., and Dikic, I. (2010) Ubiquitin ligase complexes: from substrate selectivity to conjugational specificity. *Biol. Chem.* **391,** 163–169
6. Pickart, C. M., and Eddins, M. J. (2004) Ubiquitin: structures, functions, mechanisms. *Biochim. Biophys. Acta* **1695,** 55–72
7. Ikeda, F., Crosetto, N., and Dikic, I. (2010) What determines the specificity and outcomes of ubiquitin signaling? *Cell* **143,** 677–681
8. Chen, Z. J., and Sun, L. J. (2009) Nonproteolytic functions of ubiquitin in cell signaling. *Mol. Cell* **33,** 275–286
9. Bianchi, K., and Meier, P. (2009) A tangled web of ubiquitin chains: breaking news in TNF-R1 signaling. *Mol. Cell* **36,** 736–742
10. Iwai, K., and Tokunaga, F. (2009) Linear polyubiquitination: a new regulator of NF-κB activation. *EMBO Reports* **10,** 706–713
11. Habelhah, H. (2010) Emerging complexity of protein ubiquitination in the NF-κB pathway. *Genes Cancer* **1,** 735–747
12. Liu, S., and Chen, Z. J. (2011) Expanding role of ubiquitination in NF-κB signaling. *Cell Res.* **21,** 6–21
13. Wu, X., and Karin, M. (2015) Emerging roles of Lys63-linked polyubiquitylation in immune responses. *Immunol. Rev.* **266,** 161–174
14. Akira, S., Takeda, K., and Kaisho, T. (2001) Toll-like receptors: critical proteins linking innate and acquired immunity. *Nat. Immunol.* **2,** 675–680
15. Chen, G., and Goeddel, D. V. (2002) TNF-R1 signaling: a beautiful pathway. *Science* **296,** 1634–1635
16. Dunne, A., and O'Neill, L. A. (2003) The interleukin-1 receptor/Toll-like receptor superfamily: signal transduction during inflammation and host defense. *Sci. STKE* **2003,** re3
17. Skaug, B., Jiang, X., and Chen, Z. J. (2009) The role of ubiquitin in NF-κB regulatory pathways. *Annu. Rev. Biochem.* **78,** 769–796
18. Davis, M. E., and Gack, M. U. (2015) Ubiquitination in the antiviral immune response. *Virology* **479–480**, 52–65
19. Hayden, M. S., and Ghosh, S. (2008) Shared principles in NF-κB signal-

ing. *Cell* **132,** 344–362
20. Oeckinghaus, A., Hayden, M. S., and Ghosh, S. (2011) Crosstalk in NF-κB signaling pathways. *Nat. Immunol.* **12,** 695–708
21. Sun, S. C. (2008) Deubiquitylation and regulation of the immune response. *Nat. Rev. Immunol.* **8,** 501–511
22. Katz, E. J., Isasa, M., and Crosas, B. (2010) A new map to understand deubiquitination. *Biochem. Soc. Trans.* **38,** 21–28
23. Coornaert, B., Carpentier, I., and Beyaert, R. (2009) A20: central gatekeeper in inflammation and immunity. *J. Biol. Chem.* **284,** 8217–8221
24. Panda, S., Nilsson, J. A., and Gekara, N. O. (2015) Deubiquitinase MYSM1 regulates innate immunity through inactivation of TRAF3 and TRAF6 complexes. *Immunity* **43,** 647–659
25. Lee, E. G., Boone, D. L., Chai, S., Libby, S. L., Chien, M., Lodolce, J. P., and Ma, A. (2000) Failure to regulate TNF-induced NF-κB and cell death responses in A20-deficient mice. *Science* **289,** 2350–2354
26. Tavares, R. M., Turer, E. E., Liu, C. L., Advincula, R., Scapini, P., Rhee, L., Barrera, J., Lowell, C. A., Utz, P. J., Malynn, B. A., and Ma, A. (2010) The ubiquitin modifying enzyme A20 restricts B cell survival and prevents autoimmunity. *Immunity* **33,** 181–191
27. Jin, W., Reiley, W. R., Lee, A. J., Wright, A., Wu, X., Zhang, M., and Sun, S. C. (2007) Deubiquitinating enzyme CYLD regulates the peripheral development and naive phenotype maintenance of B cells. *J. Biol. Chem.* **282,** 15884–15893
28. Kato, M., Sanada, M., Kato, I., Sato, Y., Takita, J., Takeuchi, K., Niwa, A., Chen, Y., Nakazaki, K., Nomoto, J., Asakura, Y., Muto, S., Tamura, A., Iio, M., Akatsuka, Y., *et al.* (2009) Frequent inactivation of A20 in B-cell lymphomas. *Nature* **459,** 712–716
29. Compagno, M., Lim, W. K., Grunn, A., Nandula, S. V., Brahmachary, M., Shen, Q., Bertoni, F., Ponzoni, M., Scandurra, M., Califano, A., Bhagat, G., Chadburn, A., Dalla-Favera, R., and Pasqualucci, L. (2009) Mutations of multiple genes cause deregulation of NF-κB in diffuse large B-cell lymphoma. *Nature* **459,** 717–721
30. Honma, K., Tsuzuki, S., Nakagawa, M., Tagawa, H., Nakamura, S., Morishima, Y., and Seto, M. (2009) TNFAIP3/A20 functions as a novel tumor suppressor gene in several subtypes of non-Hodgkin lymphomas. *Blood* **114,** 2467–2475
31. Yang, Y., and Staudt, L. M. (2015) Protein ubiquitination in lymphoid malignancies. *Immunol. Rev.* **263,** 240–256
32. Spain, B. H., Bowdish, K. S., Pacal, A. R., Staub, S. F., Koo, D., Chang, C. Y., Xie, W., and Colicelli, J. (1996) Two human cDNAs, including a homolog of *Arabidopsis* FUS6 (COP11), suppress G-protein- and mitogen-activated protein kinase-mediated signal transduction in yeast and mammalian cells. *Mol. Cell. Biol.* **16,** 6698–6706
33. Cardamone, M. D., Krones, A., Tanasa, B., Taylor, H., Ricci, L., Ohgi, K. A., Glass, C. K., Rosenfeld, M. G., and Perissi, V. (2012) A protective strategy against hyperinflammatory responses requiring the nontranscriptional actions of GPS2. *Mol. Cell* **46,** 91–104
34. Jakobsson, T., Venteclef, N., Toresson, G., Damdimopoulos, A. E., Ehrlund, A., Lou, X., Sanyal, S., Steffensen, K. R., Gustafsson, J. A., and Treuter, E. (2009) GPS2 is required for cholesterol efflux by triggering histone demethylation, LXR recruitment, and coregulator assembly at the ABCG1 locus. *Mol. Cell* **34,** 510–518
35. Toubal, A., Clément, K., Fan, R., Ancel, P., Pelloux, V., Rouault, C., Veyrie, N., Hartemann, A., Treuter, E., and Venteclef, N. (2013) SMRT-GPS2 corepressor pathway dysregulation coincides with obesity-linked adipocyte inflammation. *J. Clin. Invest.* **123,** 362–379
36. Venteclef, N., Jakobsson, T., Ehrlund, A., Damdimopoulos, A., Mikkonen, L., Ellis, E., Nilsson, L. M., Parini, P., Jänne, O. A., Gustafsson, J. A., Steffensen, K. R., and Treuter, E. (2010) GPS2-dependent corepressor/SUMO pathways govern anti-inflammatory actions of LRH-1 and LXR-beta in the hepatic acute phase response. *Genes Dev.* **24,** 381–395
37. Cardamone, M. D., Tanasa, B., Chan, M., Cederquist, C. T., Andricovich, J., Rosenfeld, M. G., and Perissi, V. (2014) GPS2/KDM4A pioneering activity regulates promoter-specific recruitment of PPARγ. *Cell Reports* **8,** 163–176
38. Fan, R., Toubal, A., Goñi, S., Drareni, K., Huang, Z., Alzaid, F., Ballaire, R., Ancel, P., Liang, N., Damdimopoulos, A., Hainault, I., Soprani, A., Aron-Wisnewsky, J., Foufelle, F., Lawrence, T., *et al.* (2016) Loss of the co-repressor GPS2 sensitizes macrophage activation upon metabolic stress induced by obesity and type 2 diabetes. *Nat. Med.* **22,** 780–791
39. Peng, Y. C., Kuo, F., Breiding, D. E., Wang, Y. F., Mansur, C. P., and Androphy, E. J. (2001) AMF1 (GPS2) modulates p53 transactivation. *Mol. Cell. Biol.* **21,** 5913–5924
40. Peng, Y. C., Breiding, D. E., Sverdrup, F., Richard, J., and Androphy, E. J. (2000) AMF-1/Gps2 binds p300 and enhances its interaction with papillomavirus E2 proteins. *J. Virol.* **74,** 5872–5879
41. Sanyal, S., Båvner, A., Haroniti, A., Nilsson, L. M., Lundåsen, T., Rehnmark, S., Witt, M. R., Einarsson, C., Talianidis, I., Gustafsson, J. A., and Treuter, E. (2007) Involvement of corepressor complex subunit GPS2 in transcriptional pathways governing human bile acid biosynthesis. *Proc. Natl. Acad. Sci. U.S.A.* **104,** 15665–15670
42. Lee, T. H., Yi, W., Griswold, M. D., Zhu, F., and Her, C. (2006) Formation of hMSH4-hMSH5 heterocomplex is a prerequisite for subsequent GPS2 recruitment. *DNA Repair* **5,** 32–42
43. Zhang, J., Kalkum, M., Chait, B. T., and Roeder, R. G. (2002) The N-CoR-HDAC3 nuclear receptor corepressor complex inhibits the JNK pathway through the integral subunit GPS2. *Mol. Cell* **9,** 611–623
44. Zhang, D., Harry, G. J., Blackshear, P. J., and Zeldin, D. C. (2008) G-protein pathway suppressor 2 (GPS2) interacts with the regulatory factor X4 variant 3 (RFX4_v3) and functions as a transcriptional co-activator. *J. Biol. Chem.* **283,** 8580–8590
45. Guo, C., Li, Y., Gow, C. H., Wong, M., Zha, J., Yan, C., Liu, H., Wang, Y., Burris, T. P., and Zhang, J. (2015) The optimal corepressor function of nuclear receptor corepressor (NCoR) for peroxisome proliferator-activated receptor γ requires G-protein pathway suppressor 2. *J. Biol. Chem.* **290,** 3666–3679
46. Cheng, X., and Kao, H. Y. (2009) G protein pathway suppressor 2 (GPS2) is a transcriptional corepressor important for estrogen receptor α-mediated transcriptional regulation. *J. Biol. Chem.* **284,** 36395–36404
47. Diederichs, S., Bäumer, N., Ji, P., Metzelder, S. K., Idos, G. E., Cauvet, T., Wang, W., Möller, M., Pierschalski, S., Gromoll, J., Schrader, M. G., Koeffler, H. P., Berdel, W. E., Serve, H., and Müller-Tidow, C. (2004) Identification of interaction partners and substrates of the cyclin A1-CDK2 complex. *J. Biol. Chem.* **279,** 33727–33741
48. Rickert, R. C., Roes, J., and Rajewsky, K. (1997) B lymphocyte-specific, Cre-mediated mutagenesis in mice. *Nucleic Acids Res.* **25,** 1317–1318
49. Dengler, H. S., Baracho, G. V., Omori, S. A., Bruckner, S., Arden, K. C., Castrillon, D. H., DePinho, R. A., and Rickert, R. C. (2008) Distinct functions for the transcription factor Foxo1 at various stages of B cell differentiation. *Nat. Immunol.* **9,** 1388–1398
50. Szydlowski, M., Jablonska, E., and Juszczynski, P. (2014) FOXO1 transcription factor: a critical effector of the PI3K-AKT axis in B-cell development. *Int. Rev. Immunol.* **33,** 146–157
51. Minegishi, Y., Rohrer, J., Coustan-Smith, E., Lederman, H. M., Pappu, R., Campana, D., Chan, A. C., and Conley, M. E. (1999) An essential role for BLNK in human B cell development. *Science* **286,** 1954–1957
52. Pappu, R., Cheng, A. M., Li, B., Gong, Q., Chiu, C., Griffin, N., White, M., Sleckman, B. P., and Chan, A. C. (1999) Requirement for B cell linker protein (BLNK) in B cell development. *Science* **286,** 1949–1954
53. Flemming, A., Brummer, T., Reth, M., and Jumaa, H. (2003) The adaptor protein SLP-65 acts as a tumor suppressor that limits pre-B cell expansion. *Nat. Immunol.* **4,** 38–43
54. Ochiai, K., Maienschein-Cline, M., Mandal, M., Triggs, J. R., Bertolino, E., Sciammas, R., Dinner, A. R., Clark, M. R., and Singh, H. (2012) A self-reinforcing regulatory network triggered by limiting IL-7 activates pre-BCR signaling and differentiation. *Nat. Immunol.* **13,** 300–307
55. Chow, K. T., Timblin, G. A., McWhirter, S. M., and Schlissel, M. S. (2013) MK5 activates Rag transcription via Foxo1 in developing B cells. *J. Exp. Med.* **210,** 1621–1634
56. Wasserman, R., Li, Y. S., and Hardy, R. R. (1995) Differential expression of the blk and ret tyrosine kinases during B lineage development is dependent on Ig rearrangement. *J. Immunol.* **155,** 644–651
57. Schmidt-Supprian, M., Wunderlich, F. T., and Rajewsky, K. (2007) Excision of the Frt-flanked neo (R) cassette from the CD19cre knock-in transgene reduces Cre-mediated recombination. *Trans-*

genic Res. **16,** 657–660
58. Allman, D., and Pillai, S. (2008) Peripheral B cell subsets. *Curr. Opin. Immunol.* **20,** 149–157
59. Qiu, P., Simonds, E. F., Bendall, S. C., Gibbs, K. D., Jr, Bruggner, R. V., Linderman, M. D., Sachs, K., Nolan, G. P., and Plevritis, S. K. (2011) Extracting a cellular hierarchy from high-dimensional cytometry data with SPADE. *Nat. Biotechnol.* **29,** 886–891
60. Zhang, X. (2013) Regulatory functions of innate-like B cells. *Cell. Mol. Immunol.* **10,** 113–121
61. Landmann, R., Knopf, H. P., Link, S., Sansano, S., Schumann, R., and Zimmerli, W. (1996) Human monocyte CD14 is upregulated by lipopolysaccharide. *Infect. Immun.* **64,** 1762–1769
62. Marchant, A., Duchow, J., Delville, J. P., and Goldman, M. (1992) Lipopolysaccharide induces up-regulation of CD14 molecule on monocytes in human whole blood. *Eur. J. Immunol.* **22,** 1663–1665
63. Baer, M., Dillner, A., Schwartz, R. C., Sedon, C., Nedospasov, S., and Johnson, P. F. (1998) Tumor necrosis factor α transcription in macrophages is attenuated by an autocrine factor that preferentially induces NF-κB p50. *Mol. Cell. Biol.* **18,** 5678–5689
64. Yao, J., Mackman, N., Edgington, T. S., and Fan, S. T. (1997) Lipopolysaccharide induction of the tumor necrosis factor-α promoter in human monocytic cells: regulation by Egr-1, c-Jun, and NF-κB transcription factors. *J. Biol. Chem.* **272,** 17795–17801
65. Pulvino, M., Liang, Y., Oleksyn, D., DeRan, M., Van Pelt, E., Shapiro, J., Sanz, I., Chen, L., and Zhao, J. (2012) Inhibition of proliferation and survival of diffuse large B-cell lymphoma cells by a small-molecule inhibitor of the ubiquitin-conjugating enzyme Ubc13-Uev1A. *Blood* **120,** 1668–1677
66. Pruneda, J. N., Littlefield, P. J., Soss, S. E., Nordquist, K. A., Chazin, W. J., Brzovic, P. S., and Klevit, R. E. (2012) Structure of an E3:E2 approximately Ub Complex Reveals an Allosteric Mechanism Shared among RING/U-box Ligases. *Mol. Cell* **47,** 933–942
67. Branigan, E., Plechanovová, A., Jaffray, E. G., Naismith, J. H., and Hay, R. T. (2015) Structural basis for the RING-catalyzed synthesis of K63-linked ubiquitin chains. *Nat. Struct. Mol. Biol.* **22,** 597–602
68. Maspero, E., Valentini, E., Mari, S., Cecatiello, V., Soffientini, P., Pasqualato, S., and Polo, S. (2013) Structure of a ubiquitin-loaded HECT ligase reveals the molecular basis for catalytic priming. *Nat. Struct. Mol. Biol.* **20,** 696–701
69. Pillai, S., and Cariappa, A. (2009) The follicular versus marginal zone B lymphocyte cell fate decision. *Nat. Rev. Immunol.* **9,** 767–777
70. Saito, T., Chiba, S., Ichikawa, M., Kunisato, A., Asai, T., Shimizu, K., Yamaguchi, T., Yamamoto, G., Seo, S., Kumano, K., Nakagami-Yamaguchi, E., Hamada, Y., Aizawa, S., and Hirai, H. (2003) Notch2 is preferentially expressed in mature B cells and indispensable for marginal zone B lineage development. *Immunity* **18,** 675–685
71. Moran, S. T., Cariappa, A., Liu, H., Muir, B., Sgroi, D., Boboila, C., and Pillai, S. (2007) Synergism between NF-κB1/p50 and Notch2 during the development of marginal zone B lymphocytes. *J. Immunol.* **179,** 195–200
72. Cariappa, A., Tang, M., Parng, C., Nebelitskiy, E., Carroll, M., Georgopoulos, K., and Pillai, S. (2001) The follicular versus marginal zone B lymphocyte cell fate decision is regulated by Aiolos, Btk, and CD21. *Immunity* **14,** 603–615
73. Witt, C. M., Won, W. J., Hurez, V., and Klug, C. A. (2003) Notch2 haploinsufficiency results in diminished B1 B cells and a severe reduction in marginal zone B cells. *J. Immunol.* **171,** 2783–2788
74. Jiang, X. X., Chou, Y., Jones, L., Wang, T., Sanchez, S., Huang, X. F., Zhang, L., Wang, C., and Chen, S. Y. (2015) Epigenetic regulation of antibody responses by the histone H2A deubiquitinase MYSM1. *Sci. Rep.* **5,** 13755
75. Jiang, X. X., Nguyen, Q., Chou, Y., Wang, T., Nandakumar, V., Yates, P., Jones, L., Wang, L., Won, H., Lee, H. R., Jung, J. U., Müschen, M., Huang, X. F., and Chen, S. Y. (2011) Control of B cell development by the histone H2A deubiquitinase MYSM1. *Immunity* **35,** 883–896
76. Wiener, R., Zhang, X., Wang, T., and Wolberger, C. (2012) The mechanism of OTUB1-mediated inhibition of ubiquitination. *Nature* **483,** 618–622
77. Juang, Y. C., Landry, M. C., Sanches, M., Vittal, V., Leung, C. C., Ceccarelli, D. F., Mateo, A. R., Pruneda, J. N., Mao, D. Y., Szilard, R. K., Orlicky, S., Munro, M., Brzovic, P. S., Klevit, R. E., Sicheri, F., *et al.* (2012) OTUB1 co-opts Lys48-linked ubiquitin recognition to suppress E2 enzyme function. *Mol. Cell* **45,** 384–397
78. Sato, Y., Yamagata, A., Goto-Ito, S., Kubota, K., Miyamoto, R., Nakada, S., and Fukai, S. (2012) Molecular basis of Lys-63-linked polyubiquitination inhibition by the interaction between human deubiquitinating enzyme OTUB1 and ubiquitin-conjugating enzyme UBC13. *J. Biol. Chem.* **287,** 25860–25868
79. Aggarwal, B. B., Shishodia, S., Sandur, S. K., Pandey, M. K., and Sethi, G. (2006) Inflammation and cancer: how hot is the link? *Biochem. Pharmacol.* **72,** 1605–1621
80. Karin, M. (2009) NF-κB as a critical link between inflammation and cancer. *Cold Spring Harb. Perspect. Biol.* **1,** a000141
81. Cilloni, D., Martinelli, G., Messa, F., Baccarani, M., and Saglio, G. (2007) Nuclear factor κB as a target for new drug development in myeloid malignancies. *Haematologica* **92,** 1224–1229
82. Weigert, O., and Weinstock, D. M. (2012) The evolving contribution of hematopoietic progenitor cells to lymphomagenesis. *Blood* **120,** 2553–2561
83. Sun, S. C., and Ballard, D. W. (1999) Persistent activation of NF-κB by the tax transforming protein of HTLV-1: hijacking cellular IκB kinases. *Oncogene* **18,** 6948–6958
84. Jin, D. Y., Teramoto, H., Giam, C. Z., Chun, R. F., Gutkind, J. S., and Jeang, K. T. (1997) A human suppressor of c-Jun N-terminal kinase 1 activation by tumor necrosis factor α. *J. Biol. Chem.* **272,** 25816–25823
85. Chun, A. C., Zhou, Y., Wong, C. M., Kung, H. F., Jeang, K. T., and Jin, D. Y. (2000) Coiled-coil motif as a structural basis for the interaction of HTLV type 1 Tax with cellular cofactors. *AIDS Res. Hum. Retroviruses* **16,** 1689–1694
86. Ho, Y. K., Zhi, H., Bowlin, T., Dorjbal, B., Philip, S., Zahoor, M. A., Shih, H. M., Semmes, O. J., Schaefer, B., Glover, J. N., and Giam, C. Z. (2015) HTLV-1 tax stimulates ubiquitin E3 ligase, ring finger protein 8, to assemble lysine 63-linked polyubiquitin chains for TAK1 and IKK activation. *PLoS Pathog.* **11,** e1005102
87. Pugh, T. J., Weeraratne, S. D., Archer, T. C., Pomeranz Krummel, D. A., Auclair, D., Bochicchio, J., Carneiro, M. O., Carter, S. L., Cibulskis, K., Erlich, R. L., Greulich, H., Lawrence, M. S., Lennon, N. J., McKenna, A., Meldrim, J., *et al.* (2012) Medulloblastoma exome sequencing uncovers subtype-specific somatic mutations. *Nature* **488,** 106–110
88. Cancer Genome Atlas Network (2012) Comprehensive molecular portraits of human breast tumours. *Nature* **490,** 61–70
89. Fabris, S., Mosca, L., Todoerti, K., Cutrona, G., Lionetti, M., Intini, D., Matis, S., Colombo, M., Agnelli, L., Gentile, M., Spriano, M., Callea, V., Festini, G., Molica, S., Lambertenghi Deliliers, G., *et al.* (2008) Molecular and transcriptional characterization of 17p loss in B-cell chronic lymphocytic leukemia. *Genes Chromosomes Cancer* **47,** 781–793
90. Haslinger, C., Schweifer, N., Stilgenbauer, S., Döhner, H., Lichter, P., Kraut, N., Stratowa, C., and Abseher, R. (2004) Microarray gene expression profiling of B-cell chronic lymphocytic leukemia subgroups defined by genomic aberrations and VH mutation status. *J. Clin. Oncol.* **22,** 3937–3949
91. Shah, S. P., Roth, A., Goya, R., Oloumi, A., Ha, G., Zhao, Y., Turashvili, G., Ding, J., Tse, K., Haffari, G., Bashashati, A., Prentice, L. M., Khattra, J., Burleigh, A., Yap, D., *et al.* (2012) The clonal and mutational evolution spectrum of primary triple-negative breast cancers. *Nature* **486,** 395–399
92. Stephens, P. J., Tarpey, P. S., Davies, H., Van Loo, P., Greenman, C., Wedge, D. C., Nik-Zainal, S., Martin, S., Varela, I., Bignell, G. R., Yates, L. R., Papaemmanuil, E., Beare, D., Butler, A., Cheverton, A., *et al.* (2012) The landscape of cancer genes and mutational processes in breast cancer. *Nature* **486,** 400–404
93. Banerji, S., Cibulskis, K., Rangel-Escareno, C., Brown, K. K., Carter, S. L., Frederick, A. M., Lawrence, M. S., Sivachenko, A. Y., Sougnez, C., Zou, L., Cortes, M. L., Fernandez-Lopez, J. C., Peng, S., Ardlie, K. G., Auclair, D., *et al.* (2012) Sequence analysis of mutations and translocations across breast cancer subtypes. *Nature* **486,** 405–409
94. Ciriello, G., Gatza, M. L., Beck, A. H., Wilkerson, M. D., Rhie, S. K., Pastore, A., Zhang, H., McLellan, M., Yau, C., Kandoth, C., Bowlby, R.,

Shen, H., Hayat, S., Fieldhouse, R., Lester, S. C., *et al.* (2015) Comprehensive molecular portraits of invasive lobular breast cancer. *Cell* **163,** 506–519
95. Yamamoto, M., Okamoto, T., Takeda, K., Sato, S., Sanjo, H., Uematsu, S., Saitoh, T., Yamamoto, N., Sakurai, H., Ishii, K. J., Yamaoka, S., Kawai, T., Matsuura, Y., Takeuchi, O., and Akira, S. (2006) Key function for the Ubc13 E2 ubiquitin-conjugating enzyme in immune receptor signaling. *Nat. Immunol.* **7,** 962–970
96. Ruland, J., Duncan, G. S., Wakeham, A., and Mak, T. W. (2003) Differential requirement for Malt1 in T and B cell antigen receptor signaling. *Immunity* **19,** 749–758
97. Kobayashi, T., Kim, T. S., Jacob, A., Walsh, M. C., Kadono, Y., Fuentes-Pananá, E., Yoshioka, T., Yoshimura, A., Yamamoto, M., Kaisho, T., Akira, S., Monroe, J. G., and Choi, Y. (2009) TRAF6 is required for generation of the B-1a B cell compartment as well as T cell-dependent and -independent humoral immune responses. *PLoS One* **4,** e4736
98. Touma, M., Keskin, D. B., Shiroki, F., Saito, I., Koyasu, S., Reinherz, E. L., and Clayton, L. K. (2011) Impaired B cell development and function in the absence of IκBNS. *J. Immunol.* **187,** 3942–3952
99. Ori, D., Kato, H., Sanjo, H., Tartey, S., Mino, T., Akira, S., and Takeuchi, O. (2013) Essential roles of K63-linked polyubiquitin-binding proteins TAB2 and TAB3 in B cell activation via MAPKs. *J. Immunol.* **190,** 4037–4045
100. Chu, Y., Vahl, J. C., Kumar, D., Heger, K., Bertossi, A., Wójtowicz, E., Soberon, V., Schenten, D., Mack, B., Reutelshöfer, M., Beyaert, R., Amann, K., van Loo, G., and Schmidt-Supprian, M. (2011) B cells lacking the tumor suppressor TNFAIP3/A20 display impaired differentiation and hyperactivation and cause inflammation and autoimmunity in aged mice. *Blood* **117,** 2227–2236
101. Giltiay, N. V., Chappell, C. P., Sun, X., Kolhatkar, N., Teal, T. H., Wiedeman, A. E., Kim, J., Tanaka, L., Buechler, M. B., Hamerman, J. A., Imanishi-Kari, T., Clark, E. A., and Elkon, K. B. (2013) Overexpression of TLR7 promotes cell-intrinsic expansion and autoantibody production by transitional T1 B cells. *J. Exp. Med.* **210,** 2773–2789
102. Wang, J. H., Avitahl, N., Cariappa, A., Friedrich, C., Ikeda, T., Renold, A., Andrikopoulos, K., Liang, L., Pillai, S., Morgan, B. A., and Georgopoulos, K. (1998) Aiolos regulates B cell activation and maturation to effector state. *Immunity* **9,** 543–553
103. Jumaa, H., Wollscheid, B., Mitterer, M., Wienands, J., Reth, M., and Nielsen, P. J. (1999) Abnormal development and function of B lymphocytes in mice deficient for the signaling adaptor protein SLP-65. *Immunity* **11,** 547–554
104. Notley, C. A., Baker, N., and Ehrenstein, M. R. (2010) Secreted IgM enhances B cell receptor signaling and promotes splenic but impairs peritoneal B cell survival. *J. Immunol.* **184,** 3386–3393
105. Lino, A. C., Mohr, E., and Demengeot, J. (2013) Naturally secreted immunoglobulins limit B1 and MZ B-cell numbers through a microbiota-independent mechanism. *Blood* **122,** 209–218
106. DeFuria, J., Belkina, A. C., Jagannathan-Bogdan, M., Snyder-Cappione, J., Carr, J. D., Nersesova, Y. R., Markham, D., Strissel, K. J., Watkins, A. A., Zhu, M., Allen, J., Bouchard, J., Toraldo, G., Jasuja, R., Obin, M. S., *et al.* (2013) B cells promote inflammation in obesity and type 2 diabetes through regulation of T-cell function and an inflammatory cytokine profile. *Proc. Natl. Acad. Sci. U.S.A.* **110,** 5133–5138
107. Kotecha, N., Krutzik, P. O., and Irish, J. M. (2010) Web-based analysis and publication of flow cytometry experiments. *Curr. Protoc. Cytom.* Chapter 10, Unit 10.17
108. Horikawa, M., Minard-Colin, V., Matsushita, T., and Tedder, T. F. (2011) Regulatory B cell production of IL-10 inhibits lymphoma depletion during CD20 immunotherapy in mice. *J. Clin. Invest.* **121,** 4268–4280
109. Langmead, B., Trapnell, C., Pop, M., and Salzberg, S. L. (2009) Ultrafast and memory-efficient alignment of short DNA sequences to the human genome. *Genome Biol.* **10,** R25
110. Li, B., and Dewey, C. N. (2011) RSEM: accurate transcript quantification from RNA-Seq data with or without a reference genome. *BMC Bioinformatics* **12,** 323
111. Cederquist, C. T., Lentucci, C., Martinez-Calejman, C., Hayashi, V., Orofino, J., Guertin, D., Fried, S. K., Lee, M.-J., Cardamone, M. D., and Perissi, V. (2017) Systemic insulin sensitivity is regulated by GPS2 inhibition of AKT ubiquitination and activation in adipose tissue. *Mol. Metab.* **6,** 125–137

Inhibition of Ubc13-mediated Ubiquitination by GPS2 Regulates Multiple Stages of B Cell Development

Claudia Lentucci, Anna C. Belkina, Carly T. Cederquist, Michelle Chan, Holly E. Johnson, Sherry Prasad, Amanda Lopacinski, Barbara S. Nikolajczyk, Stefano Monti, Jennifer Snyder-Cappione, Bogdan Tanasa, M. Dafne Cardamone and Valentina Perissi

J. Biol. Chem. 2017, 292:2754-2772.
doi: 10.1074/jbc.M116.755132 originally published online December 30, 2016
